2013

Looping RAFOS floats in the California Current System

Collins, Curtis A.

þÿ Deep-Sea Research II, Volume 85, (2013), pp. 42 61
http://hdl.handle.net/10945/43247

Deep-Sea Research II 85 (2013) 42–61

Contents lists available at SciVerse ScienceDirect

Deep-Sea Research II

journal homepage: www.elsevier.com/locate/dsr2

Looping RAFOS floats in the California Current System

Curtis A. Collins *, Tetyana Margolina, Thomas A. Rago, Leonid Ivanov

Department of Oceanography, Naval Postgraduate School, Monterey, CA, United States

ARTICLE INFO

Available online 27 July 2012

Keywords:
Isobaric floats
California Undercurrent
California Current
Mesoscale eddies
Meddies
Topographic drag

ABSTRACT

Looping motions of RAFOS floats deployed off the Central California coast between 1992 and 2010 are described. Most floats were deployed in the California Undercurrent. Floats at 300 m were observed to loop 26% of the time, with anticyclonic rotation observed about twice as often as cyclonic rotation. Characteristics of anticyclonic rotation at 300 m included median swirl speeds of 14 cm/s for diameters of 59 km and 14-day periods. Long-lived (>70 days and at least 8 consecutive loops) anticyclonic loopers are identified as *C*alifornia *U*ndercurrent e*ddies* (or "cuddies"). One cuddy was observed to move southwestward 1650 km over a period of 520 days before observations ended. Kinematically, cuddies are similar to Mediterranean Water eddies (meddies) in the Iberian Basin, except that meddies are somewhat stronger, larger and deeper.

Over the slope, most cuddies were formed between either Pt. Sur and Pt. Reyes or Cape Mendocino and Cape Blanco. The region north of Cape Mendocino is estimated to generate six cuddies each year. These eddies form from waters on the inshore side of the California Undercurrent as they move past Cape Mendocino. Topographic drag is the most likely formation mechanism.

Two of eight deep floats were observed to loop, one anticyclonically (1545 m) for 279 days and the other cyclonically (1167 m) for 192 days. Looping for these floats ended near Taney Seamounts.

Published by Elsevier Ltd.

1. Introduction

Subsurface circulation patterns associated with the inshore portion of the California Current System have been observed using isobaric RAFOS floats (Rossby et al., 1986) from 1992 to 2011. Garfield et al. (1999) studied the first four years of this data set, noting that anticyclonic motion accompanied by slow westward drift was the dominant mode of float variability to the west of the California Undercurrent (CUC), which carries equatorial waters poleward along the continental slope. In this paper the entire data set of RAFOS observations is used to identify the floats that exhibit looping behavior and to describe their characteristics.

Most floats were launched at a depth of 300 m over the continental slope along the Central California coast. At this depth, the poleward flowing CUC dominates the circulation to a distance of about 100 km from the coast. The CUC is a deep current, extending to at least 1000 m, with largest mean velocity, 10 cm/s, at a depth of 100 m (Collins et al., 2000). The CUC varies seasonally, and the subsurface maximum is in part because the shallow inshore edge of the California Current lies above the CUC in spring and summer. Current meter measurements over a six year period showed that weekly velocities of the CUC at a depth of 350 m off Pt. Sur were minimum (3 cm/s) in March and October, and maximum (16 cm/s) in May (Collins et al., 1996). The CUC carried the RAFOS floats poleward. Hence, observed looping motion included the area along the entire West Coast of the United States between 30°N and ~48°N (from about Pt. Conception, California, to Cape Flattery, Washington) and from 115°W to 140°W. This is also a region of complex topography, including coastal capes, escarpments, seamounts, and submarine canyons.

Other studies have noted that this is a region of high mesoscale variability. (See, for example, the first synoptic surveys of the California Current off Pt. Conception [Sverdrup, 1939].) Recent analyses of moored current arrays (Chereskin et al., 2000) and sea surface height anomalies from satellite altimeters (Chelton et al., 2011; Ivanov et al., 2010; Keister and Strub, 2008) confirm that the California Current System is a region of rich mesoscale activity including eddies, fronts, filaments and Rossby waves. Chelton et al. (2011), in a study of global SSH anomalies, note that Eastern Boundary currents are a region of eddy generation. The RAFOS trajectories reported here provide a Lagrangian view of the subsurface eddy field that complements other data by revealing flow paths and dispersion patterns. The trajectories also suggest how eddies are generated.

In order to compare results with previous studies, Richardson's (1993) definition of a looping float (looper) is used: a float must make at least two consecutive loops in the same direction.

* Corresponding author. Tel.: +1 831 656 3271.
E-mail address: collins@nps.edu (C.A. Collins).

0967-0645/$ - see front matter Published by Elsevier Ltd.
http://dx.doi.org/10.1016/j.dsr2.2012.07.027

Although there are several possible causes for looping motion, loopers are usually identified with moving coherent structures: Rossby-like waves, mesoscale and submesoscale eddies, coastally trapped waves, etc. (Flierl, 1981; Regier and Stommel, 1979). For example, Regier and Stommel (1979) demonstrated that looping float trajectories are observed in linear waves propagating on a mean current. In previous studies of subsets of our CUC RAFOS float data, Garfield et al. (1999) detected only anticyclonic looping and identified the eddies that caused this motion as CUC eddies or "cuddies" because their core contained CUC waters. Collins et al. (2004) demonstrated that cuddies represented a sub-diffusion dispersion of RAFOS floats. Margolina et al. (2006) identified both cyclonically and anticyclonically looping floats and tabulated kinematic properties of the anticyclonic eddies. Note that Lukas and Santiago-Mandujano (2001) found extreme anomalous water properties north of Oahu that likely originated in an anticyclonic eddy off Baja California, corresponding to a propagation distance of at least 4600 km.

The paper is organized as follows: Section 2 contains description of the RAFOS data used in this study, while Section 3 describes filtering and smoothing of original trajectories, separation of float motion into rotational and translation components, and calculation of the kinematic characteristics for the looping floats. Results are described and discussed in Section 4. Finally, Section 5 summarizes results and compares the properties of anticyclonic eddies reported here to those of meddies.

2. Data

Deployment of quasi-isobaric RAFOS floats in the California Undercurrent began in 1992, with data collection ending in 2010. Observations were focused on the coastal undercurrent at about 300 dbar (subsequently referred to as shallow floats), but a few floats were launched at ~1500 dbar (subsequently referred to as deep floats). The floats were mostly launched as triads prior to 2001 across the continental slope along the Central California coast between 36°N and 38°N on cruises of opportunity. Observational details including source locations, time and location of float launch, and navigation methods and accuracy were described in Margolina et al. (2006). Processed float data may be obtained from http://www.oc.nps.edu/npsRAFOS/.

The most serious limitation of the floats as an indicator of Lagrangian motion was that they did not precisely follow parcels of water. This is because the floats are quasi-isobaric, whereas water parcels move along surfaces of neutral density (isopycnals). The density of a RAFOS float varied due to in situ temperature changes, which in turn modified the float density because of the differing thermal expansions of the glass hull and aluminum end cap. These float density changes in the NE Pacific resulted in a float's sinking when it warmed and rising when it cooled, exactly opposite to the way a water parcel would behave (Swift and Riser, 1994). An estimate of the magnitude of this effect can be obtained from float pressure measurements: for those floats which did not leak, the mean (median) standard deviation of the pressure along the float trajectory was 26 (17) dbar for all shallow floats.

Position error varied with the geometry of source and float locations. The absolute uncertainty in position for each float was estimated to be less than 10 km (Garfield et al., 1999). J. Gobat (personal communication, 2005) used the same sources as the RAFOS floats described below to navigate a sea glider equipped with a hydrophone and RAFOS processor. He measured RMS position errors between glider navigation and RAFOS positions of 2.4 km. Absolute position error is important when comparing the position of one float to the position of another float, sea surface features determined by altimetry, shipboard measurements, the coastline, etc. The precision of the absolute position error is more relevant to the calculation of looper properties, and this has been estimated to be ± 1 km over a period of one month for distances of less than 200 km (Garfield et al., 1999).

A final bias in our measurements was due to the floats being launched unevenly throughout the year, leaving the seasonal cycle poorly resolved. This issue is discussed below. This is relevant because CUC measurements (Collins et al., 1996, 2004) show a strengthening of the current in spring. To the extent that this strengthening contributes to increased instability or topographic drag, rates of eddy formation may have been biased.

3. Methods

Sampling rates for looping RAFOS floats varied from one (~55% of loopers) to two (~32% of loopers) and three (~13%) samples per day, and four floats sampled two or three times per day every other day. The sampling frequency decreased as the observation program matured, resulting in longer source and float deployments. Shallow (deep) float missions were set at 825 (1200) days after 2003. The low sampling rates failed to resolve energetic higher frequency motions caused by tides and inertial waves, but were not pertinent to studying lower frequency behavior of the floats (Benson, 1995).

Recent studies of sea surface height anomalies have identified individual mesoscale features that are "long-lived" and behave as coherent vortices or eddies. To facilitate comparison between the behavior of looping floats and individual sea surface anomalies, long-lived loopers have been identified. The criteria for "long-lived" that we adopted were at least eight consecutive loops with a total duration exceeding 70 days (similar to Stegmann and Schwing, 2007). Note that numerical ocean model results have been analyzed using similar "long-lived" criteria (Kurian et al., 2011). In the case of the numerical model results, point by point comparisons are not possible; but comparsion of statistics of observed loopers and numerical loopers should be possible (Garfield et al., 2001). Long-lived anticyclonic eddies will subsequently be referred to as cuddies.

3.1. Smoothing and filtering

Position data were smoothed using cubic splines (function *spaps* in the MATLAB® Spline Toolbox). Tolerance parameters were chosen experimentally and set to one. This resulted in smoothing parameters varying between 0.15 and 0.5 for different floats, depending on sampling frequency and navigation noise. Use of cubic smoothing splines reduced unresolved motions with time scales less than a day while preserving signals with longer periods (Boebel et al., 2003). The splines had no effect on the kinematic properties of the loopers.

Looping motions were separated from lower frequency translational and rotational motions using band pass or low pass Butterworth filters. These were chosen separately for each float. For example, the normalized 3 dB cutoff frequencies for Float 73 were chosen as [0.04 0.10]. This removed motions with periods less than 10 days and more than 25 days.

3.2. Eddy kinematic characteristics

Eddy kinematic characteristics were estimated from smoothed trajectories following the procedures introduced by Richardson (1993). Eddy kinematic characteristics included: T, the period of rotation as ratio of the looping duration to the number of loops; V_S, the characteristic swirl speed as a root mean square speed of

the float relative to its mean speed; and $R=(V_S T/2\pi)$, the mean radius of the float rotation.

Note that the reliability of the radius estimates depended upon the number of loops and upon the degree to which the loop radius varied along the trajectory (Shoosmith et al., 2005).

4. Results

A total of 65 shallow floats were used in this study. Nineteen did not loop. Thirty eight (fifteen) looped anticyclonically (cyclonically), of which seven were both cyclonic and anticyclonic loopers. The duration of shallow looping was 22.1 years of the 84.7 years of float observations. This meant that the shallow floats were looping 26% of the time.

Eight deep floats are also included in this study, although additional deep float measurements at 2000 dbars near hydrothermal vents reported by Lupton et al. (1998) have been omitted. Six deep floats did not loop, one looped cyclonically and another looped anticyclonically. The duration of deep looping was 1.3 years of 14.4 years of deep float observations. The deep floats looped 9% of the time, a rate about one-third that of the shallow floats.

Non-looping floats often demonstrated behavior similar to that for Lagrangian particles in two-dimensional hydrodynamic turbulence. This behavior is characterized by chaotic motions of individual floats and rapid divergence with time of two neighboring floats (Ivanov et al., 2009).

4.1. Shallow floats

The number of observed shallow float days within a given $0.5^\circ \times 0.5^\circ$ area is shown in Fig. 1 (left). The shape and pattern of the distribution of float observations gives a rough idea of the dispersion of floats from their launch locations. Highest observation densities, >200 float days, occurred along the Central California coast where most floats were launched and extended northward along the coast to 42.5°N. As latitude decreases, the distance from shore of $0.5^\circ \times 0.5^\circ$ areas with observations increased to 34.5°N, suggesting that the total length of path from the launch (along the coast and thence offshore) was about the same for floats with similar duration. Regions with greater than 100 float days were not found to the west of 130.5°W. To the east of 130.5°W and north of 34°N there was only one 0.5° square area for which there were no data.

Nineteen of the shallow floats did not loop, while 46 exhibited looping behavior. The trajectories for these loopers are shown in Fig. 2, and their kinematic characteristics listed in Table 1 (Table 2) for anticyclonic (cyclonic) loopers. Seven floats contained both cyclonic and anticyclonic loops. Float 67 (92) contained three separate anticyclonic (cyclonic) loopers. Fourteen shallow floats that looped continuously at least eight times for more than 70 days were classified as "long-lived loopers" and identified as representing eddies. The most striking features of the looping trajectories shown in Fig. 2 were the tracks of three cuddies to the south of 40°N which extended from near the coast into the ocean interior in a westward or west-southwestward direction for about 1000 km.

Fig. 1 (right) shows the geographic distribution of shallow looping floats as a percentage of the total float observations. In the region located between the coast and 100 km offshore from Central California where the density of observations was greater than 200 float days per 0.5° square area, the percentage of looping floats was relatively low, 10% or so, which is in good agreement with the Garfield et al. (1999) observation that trajectories over the continental slope consisted of alongshore motions. In looking for areas with both a high number of float observations and a high percentage of looping floats (e.g., regions either of preferred eddy generation or with stalled or semipermanent eddies), we found that there were only a few 0.5° square areas with looper frequencies of $\sim$50%: near Davidson Seamount to the southwest of Pt. Sur, and to the north and south of Pt. Arena. Westward of 128°W, the 0.5° square areas that were occupied by loopers have high percentages but few float days.

The monthly distribution of shallow looper observations is shown in Fig. 3. Even though the floats were launched non-uniformly throughout a year, with most floats deployed in May and July to November, float days were almost evenly distributed during the year (Fig. 3A). The maximum percentage of anticyclonically looping float days occurred in November; but the percentage varied little from August to February, $\sim 22 \pm 2$%. The percentage of anticyclonic looping was about half this rate from March through June, and was minimum in May at 7% (Fig. 3B). This seasonal pattern is similar to that observed for eddy kinetic energy for these floats (Collins et al., 2004). Other observations have documented maximum eddy kinetic energy of sea surface

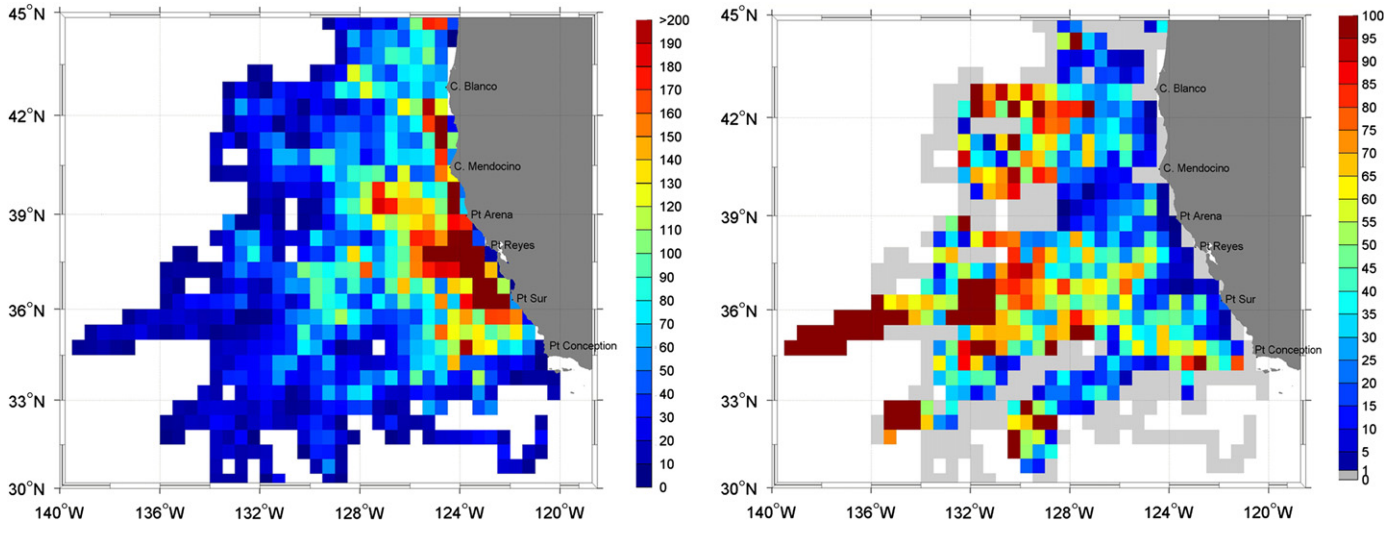

Fig. 1. (Left) The number of daily 300 m float observations per $0.5^\circ \times 0.5^\circ$ square for the period 1992–2010. (Right) Percent of the time looping floats were observed in a $0.5^\circ \times 0.5^\circ$ square during the period 1992–2010.

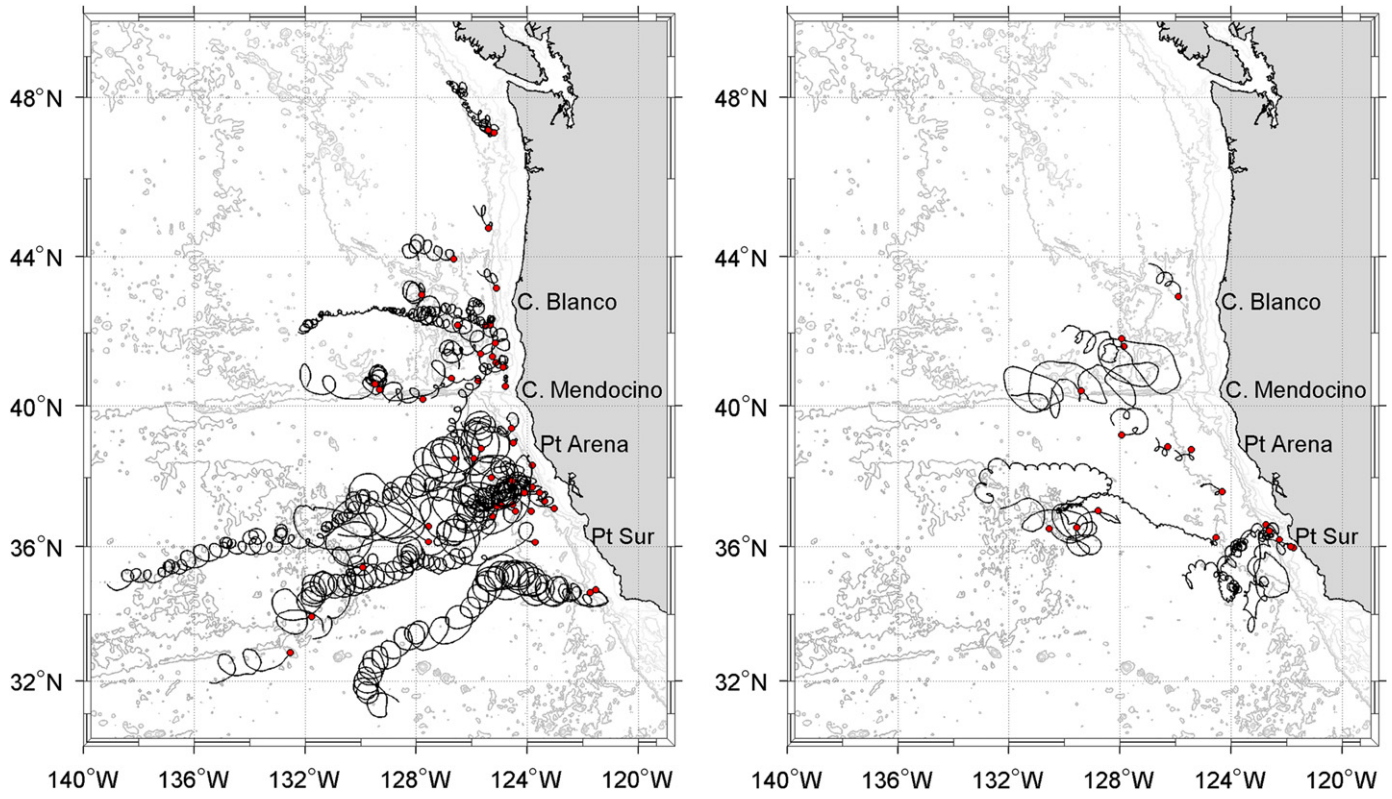

Fig. 2. Looping trajectories for anticyclonic (left) and cyclonic (right) 300 dbar RAFOS floats, 1993–2009. Red dots indicate the beginning of looping behavior. 200, 1000, 2000, 3000, 4000, and 5000 m isobaths are shown. (For interpretation of the references to color in this figure legend, the reader is referred to the web version of this article.)

height anomalies in the California Current System in the fall (Kelly et al., 1998). Chelton et al. (2011) show that long-lived eddies account for about 40% of the eddy kinetic energy variability.

Kinematic properties of anticyclonic (cyclonic) loopers are listed in Table 1 (Table 2). The total duration of anticyclonic looping by shallow floats was 15.4 years (~18% of all shallow float observations) and 6.7 years (~8% of all shallow float observations) for cyclonic looping. For anticyclonic loopers, the largest number of consecutive loops was 72 (Float 107) and the longest duration of anticyclonic looping was 520 days (Float 109). For cyclonic loopers, Float 112 had the largest number of consecutive loops, 78, for a total duration of 390 days. Cyclonic looping motion was usually of much shorter duration than anticyclonic looping motion. About 50% of the cyclonic loopers had only two loops, with only 30% making more than 10 consecutive loops. Roughly two-thirds of the cyclonic loopers originated between the end of September and the beginning of December.

4.2. Eddy formation

Launch locations and the location where the float began looping motion are shown in Fig. 4 for floats which first looped anticyclonically and Fig. 5 for floats which first looped cyclonically. The launch to start of anticyclonic looping is shown in two panels: one for floats which began looping to the north, the second for floats which began looping to the south, of Cape Mendocino. Most floats were launched over the continental slope, where their motion was constrained by bathymetry. They subsequently moved poleward or westward and then began to loop. It is important to note that the start of looping may not indicate eddy formation, as the float may become entrained in an existing eddy.

Over the continental slope, anticyclonic looping usually began either between Pt. Sur and Pt. Reyes or between Cape Mendocino and Cape Blanco (Fig. 4). Two floats (105, 106) were launched into the same eddy to the west of Pt. Conception. Over the continental slope, cyclonic looping was observed to begin only between Pt. Sur and Pt. Reyes in the months of September and October (probably due to limited sampling). In deeper waters offshore, cyclonic looping occurred over a much larger latitudinal range (Fig. 5). Four floats began cyclonic looping within a short distance of their launch site, while another four of the anticyclonic loopers behaved similarly.

Nearly 75% of the floats traveled at least 100 km before looping. Not all floats that moved poleward in the CUC became loopers. Some floats left the CUC in a complex manner defined by the mesoscale features of the nearshore and offshore circulation.

Two areas exist for a more detailed study of coastal eddy formation: Pt. Sur and Cape Mendocino. Twenty-five (twenty-four) floats were observed to pass Cape Mendocino (Pt. Sur). At Cape Mendocino, all floats were moving poleward and either moved offshore or northward at the Cape. Near Pt. Sur the situation was more complex, with five floats moving southward (three of which formed cyclonic loopers), three moving offshore, and the remainder moving poleward. Because of the complexity of alongshore float movement at Pt. Sur, the larger number of floats passing Cape Mendocino, and the fact that Garfield et al. (1999) have shown a number of examples for Cape Mendocino, it was decided to describe the formation processes and formation rates for cuddies in the Cape Mendocino region and to defer studies at Pt. Sur.

Twenty five floats were observed to approach Cape Mendocino from the south. (Float 110 transited Cape Mendocino twice.) While each transit was unique, several behaviors were repeated both with and without looping: offshore flow, interaction with coastal features

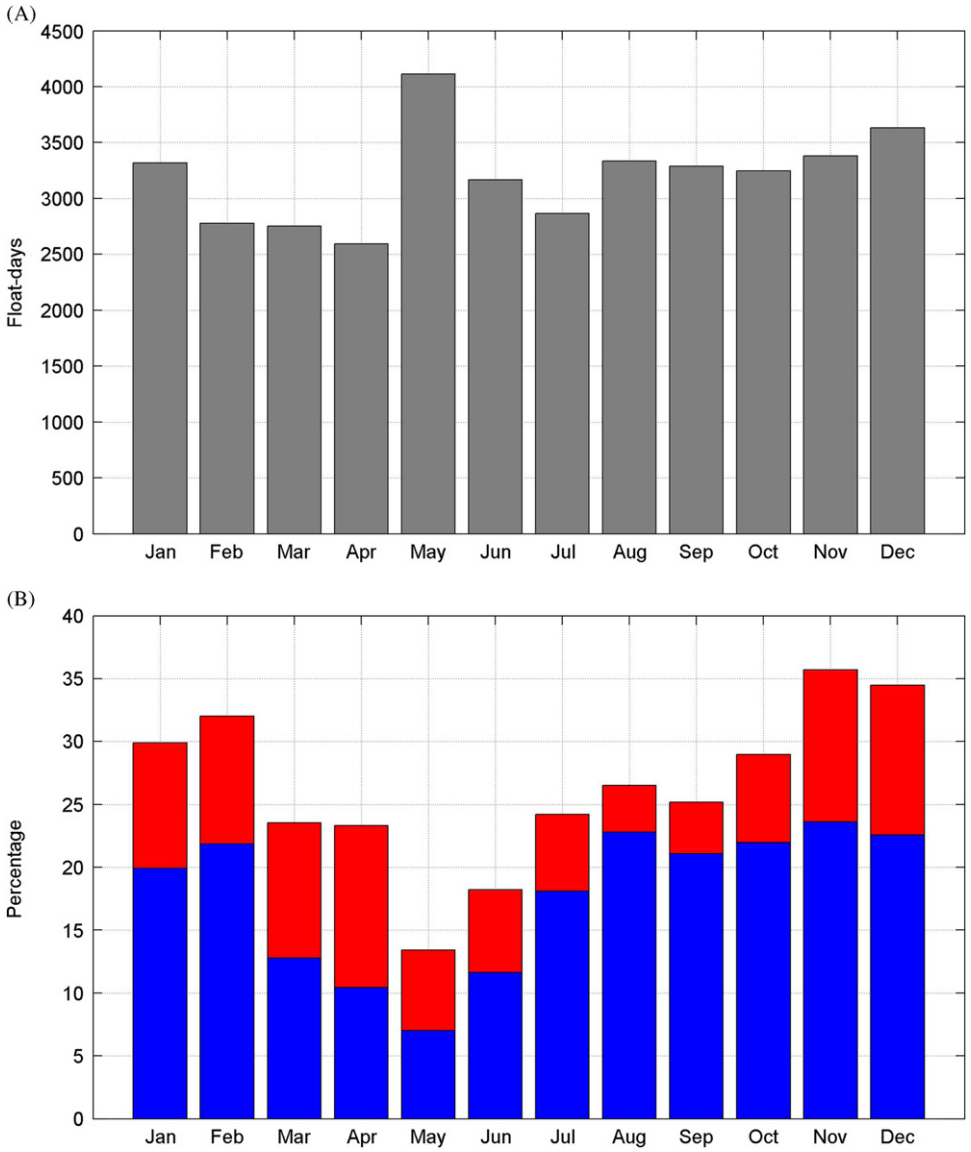

Fig. 3. Monthly distribution of float days: (A) all floats and (B) percentage of loopers relative to total number of float-days. Observations include the period from August 1992 to February 2010. Blue (red) represents anticyclonic (cyclonic) loopers. (For interpretation of the references to color in this figure legend, the reader is referred to the web version of this article.)

(reefs, submarine canyons), and epicycloidal behavior. Fourteen floats became entrained in offshore flows and eleven exhibited some interaction with the coastal region between Cape Mendocino and Cape Blanco. Eleven commenced anticyclonic looping between Cape Mendocino and Cape Blanco, including two to the west of Cape Mendocino over the Mendocino escarpment. Of the eight floats that successfully transited the coastal region between the Capes without looping, three began looping to the north of Cape Blanco. Three examples of float transit are given below for Cape Mendocino.

4.2.1. *Inshore formation of a cuddy (Float 109)*

Anticyclonic looping was observed to form over the upper slope inshore of the subsurface velocity maximum of the CUC. An example is shown in Fig. 6 for Float 109. Float 109 moved poleward in the CUC on April 26, 2005, at 40°N with a speed of 30 cm/s. As it passed to the west of Cape Mendocino on April 30, it decelerated to 15 cm/s. The trajectory of Float 109 thence continued along the upper slope and moved into Eel Canyon. It changed its course from eastward to northward on May 4, then slowed to 7 cm/s and rotated anticyclonically in an ~15 km diameter loop over the next five days. (Note that this small precursor loop was not included with the loopers in Tables 1 and 2 because it was not similar to the subsequent looping and distorted the kinematic characteristics.) Float 109 subsequently left this loop moving westward and then northward, entering the southern entrance to Trinidad Canyon two days later. In the outer reaches of Trinidad Canyon, four loops of about five days period occurred, with the diameter of the looping trajectory increasing to ~35 km. A fifth 5-day loop then carried the float to the west into water deeper than 3 km, from whence it continued its westward movement, averaging one 48 km diameter loop every 8 days (not shown in figure).

Bower et al. (1997) noted cusps in trajectories associated with rapidly translating rotary motion and referred to this feature as "epicycloidal" behavior, and this usage has been adopted here. Epicycloidal behavior was important as it was a common precursor to looping in the Iberian Basin (Bower et al. 1997). The epicycloidal character of the trajectory implies that translation is large relative to the amplitude of rotary motion. Regier and

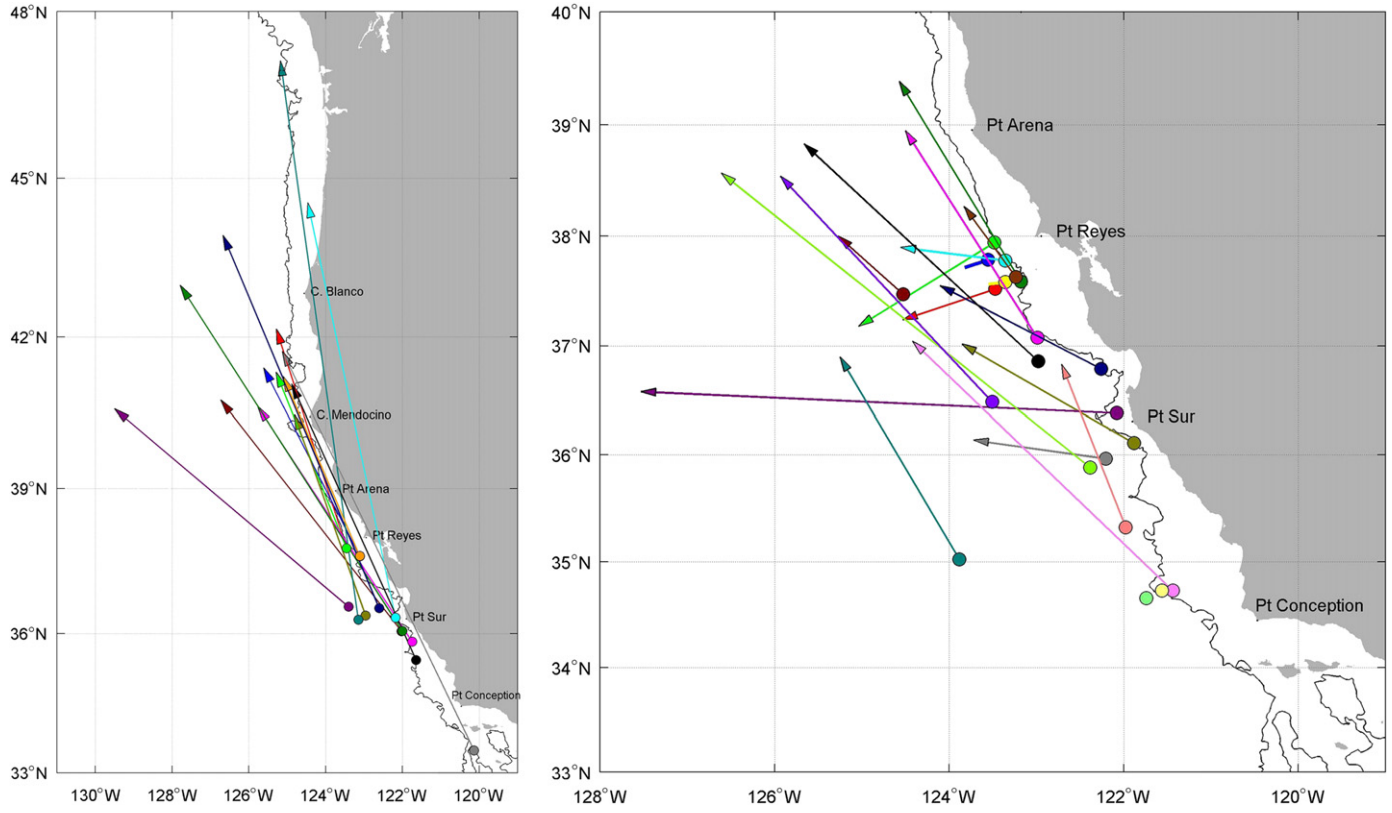

Fig. 4. Launch position (circle) and beginning of shallow anticyclonic looping (arrow). (left) Looping north of Cape Mendocino. (right) Looping south of Cape Mendocino. The light green (Float 105) and light yellow (Float 106) floats near 34.7°N, 122°W were launched into an eddy, while Floats 11 (blue) and 13 (yellow) off Pt. Reyes moved offshore only a short distance before looping commenced. Therefore, for clarity, no arrowheads are drawn for these floats.

Stommel (1979), Flierl (1981), Ivanov and Eremeev (1987), Chelton et al. (2011) and others use the ratio of the maximum rotational speed, U, and the translation speed, c, as an advective nonlinearity parameter to determine if a coherent structure (eddy or nonlinear wave or a combination of linear waves and mean flow) advects parcels of water. The values of $U/c \geq 1$ would correspond to looping behavior and imply that there is trapped fluid within the anticyclonic eddy. Ivanov and Eremeev (1987) also demonstrated that $U/c \geq 1$ is a condition of stability for a coherent structure in terms of Lagrangian representation. For Float 109, the values of U/C were less than one at the start of the trajectory shown in Fig. 6 and greater than one subsequent to May 4. The time for the pathway to transition from epicycloidal to looping behavior of Float 109 was estimated as the length of time of the float transit of the small precursor loop, which was five or six days.

D'Asaro (1988) observed that the key step in the generation of anticyclonic vortices in Barrow Canyon was the reduction in the potential vorticity of their source waters to nearly zero. He proposed that this occurred through the action of frictional torques as the source water, driven by downstream pressure gradients concentrated on the nearshore side of the canyon, flowed through the Canyon. The generation of looping behavior described above was somewhat different from vortex formation described by D'Asaro (1988). Although the looping was initiated on the inshore (anticyclonic) side of the CUC, there was considerable interaction with topography as well as the CUC. The stronger translation velocities and Coriolis force associated with the transit of Cape Mendocino took Float 109 into Eel Canyon where it slowed and rotation associated with epicycloidal motion began. The float subsequently moved to the larger Trinidad Canyon where it continued to interact with the offshore core of the CUC. The subsequent swirl speed, ~20 cm/s, was typical of float translation speeds in the CUC (Fig. 7, Garfield et al., 1999). After moving out of the Canyon, Float 109 migrated westward, due to β effects or due to offshore flows which occur in this region (Barth et al., 2000).

Coastal interaction with Cape Mendocino and Trinidad Canyon also resulted in looping behavior for Floats 89 and 107. Floats 87, 92 and 110 moved offshore but did not loop after interacting with these coastal features. Float 48 looped anticyclonically once in Eel Canyon, after which it continued without looping offshore and northward past Cape Blanco. Details of the kinematics of these floats were examined, e.g., speed of approach to Cape Mendocino, deceleration at Cape Mendocino, epicycloidal behavior, but none was a certain predictor of cuddy formation. Ambient flow conditions, not just the strength of the CUC, must govern coastal eddy generation at Cape Mendocino.

4.2.2. *Offshore formation of cuddies at Cape Mendocino (Floats 4 and 67)*

A second type of initiation of looping behavior was observed at Cape Mendocino that more closely resembles the vortex formation mechanism described by D'Asaro (1988). In this case, floats were swept offshore into deeper water to the west of Cape Mendocino. Trajectories that illustrate this behavior are shown for Floats 4 and 67 in Fig. 7. Both floats approach Cape Mendocino inshore, with Float 4 (67) moving northward across 40°N on September 27, 1993 (May 11, 1999). The floats followed the isobaths offshore to the south of Cape Mendocino, separated from the coast, and then moved offshore into deeper water at the Cape, presumably carrying anticyclonic vorticity associated with inshore CUC waters. Epicycloidal motion appeared about

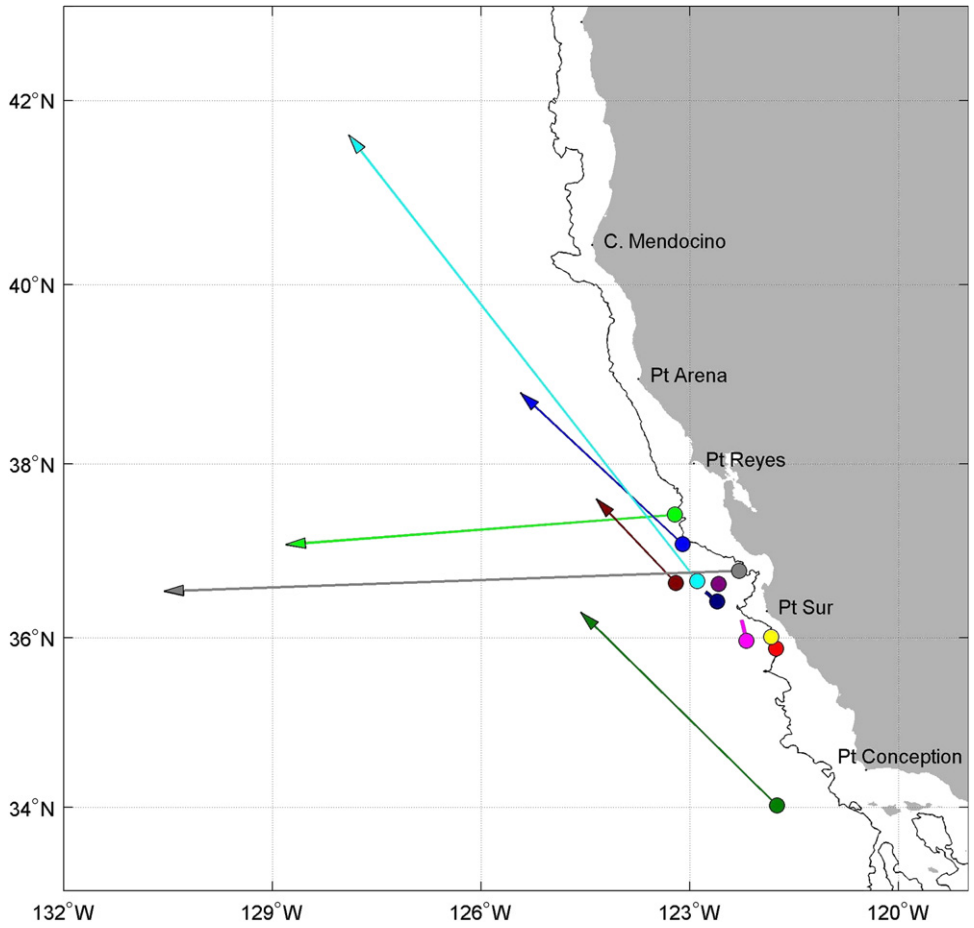

Fig. 5. Launch position (circle) and beginning of shallow cyclonic looping (arrow). Floats 29 (red), 66 (yellow), 83 (magenta), 112 (dark purple) and 111 (dark blue) moved only a short distance before looping commenced. Therefore, for clarity, no arrowheads are drawn for these floats. (For interpretation of the references to color in this figure legend, the reader is referred to the web version of this article.)

70 km to the west of Cape Mendocino with a period of about 4–5 days.

Three distinct trains of loops appear in Float 67 immediately after the first epicycloidal crest. (Note that each of these trains is represented as a separate looping event in Table 1 due to changes in the physical characteristics of the loops.) The first five loops had a period of five days, a swirl speed of 20 cm/s, a diameter of 25 km, and $U/c=2.8$. The next two loops had a period of 11 days, a swirl speed of 16.8 cm/s, a diameter of 50 km, and $U/c=3.7$. These two sets of loops took place along the Mendocino escarpment. On July 15, Float 67 stopped its trend of westward movement and began a sequence of seven loops with 13-days period, 15.4 cm/s swirl speed, 55 km diameter and $U/c\sim\infty$. Float 67 exited these loops to the southeast, crossed the Mendocino escarpment, and later moved inshore, turning northward on November 29, ending its mission 27 days later about 100 km to the west of Pt. Arena. (The last part of this trajectory is not shown in Fig. 7.)

Float 4 experienced a series of seven epicycloids or wave crests about 5 days apart as it moved west and then southwest across Mendocino escarpment. At 39°N, 131°W, Float 4 began a much larger loop, 140 km in diameter. However, the mission ended before this loop was completed; hence, Float 4 is not listed as a looper in Table 1. For Floats 4 and 67, two time scales seemed important for cuddy formation: one was the period of epicycloids, and the other was related to the time scale of the deceleration of the offshore flow. U/c ratios could not be reliably estimated for Float 4.

Floats that were experiencing epicycloidal behavior and subsequently were swept offshore at Cape Mendocino were always associated with subsequent cuddy formation. Other floats which were not behaving epicycloidally were also swept offshore and were either entrained into cuddies or formed cuddies. As noted above, floats launched after 2003 sampled only once per day, so epicycloidal behavior would have been more difficult to detect. Two floats (Floats 87, 92) moved offshore between Cape Mendocino and Cape Blanco and did not experience anticyclonic looping.

4.2.3. *Formation rate of anticyclonic eddies at Cape Mendocino*

To estimate the generation rate of anticyclonic eddies in the CUC at Cape Mendocino, we need to know either the length of time that it takes an eddy to form (capture undercurrent water in its core) or, in the case that eddy formation processes are initiated next to Cape Mendocino but the eddy actually forms offshore, how long it will take that parcel of water to move out of the region so that another eddy could form next to the coast. For the examples shown above, Float 109 took five to six days to form, and Floats 4 and 67 moved a distance of 60–80 km from Cape Mendocino in a week, a distance sufficient that the epicycloidal motions were unlikely to influence CUC waters at the Cape.

There were two instances of floats passing Cape Mendocino within a week of one another. Floats 87 and 88 moved past Cape Mendocino one week apart and had nearly identical paths around Cape Mendocino and Trinidad Canyon. Float 88 continued

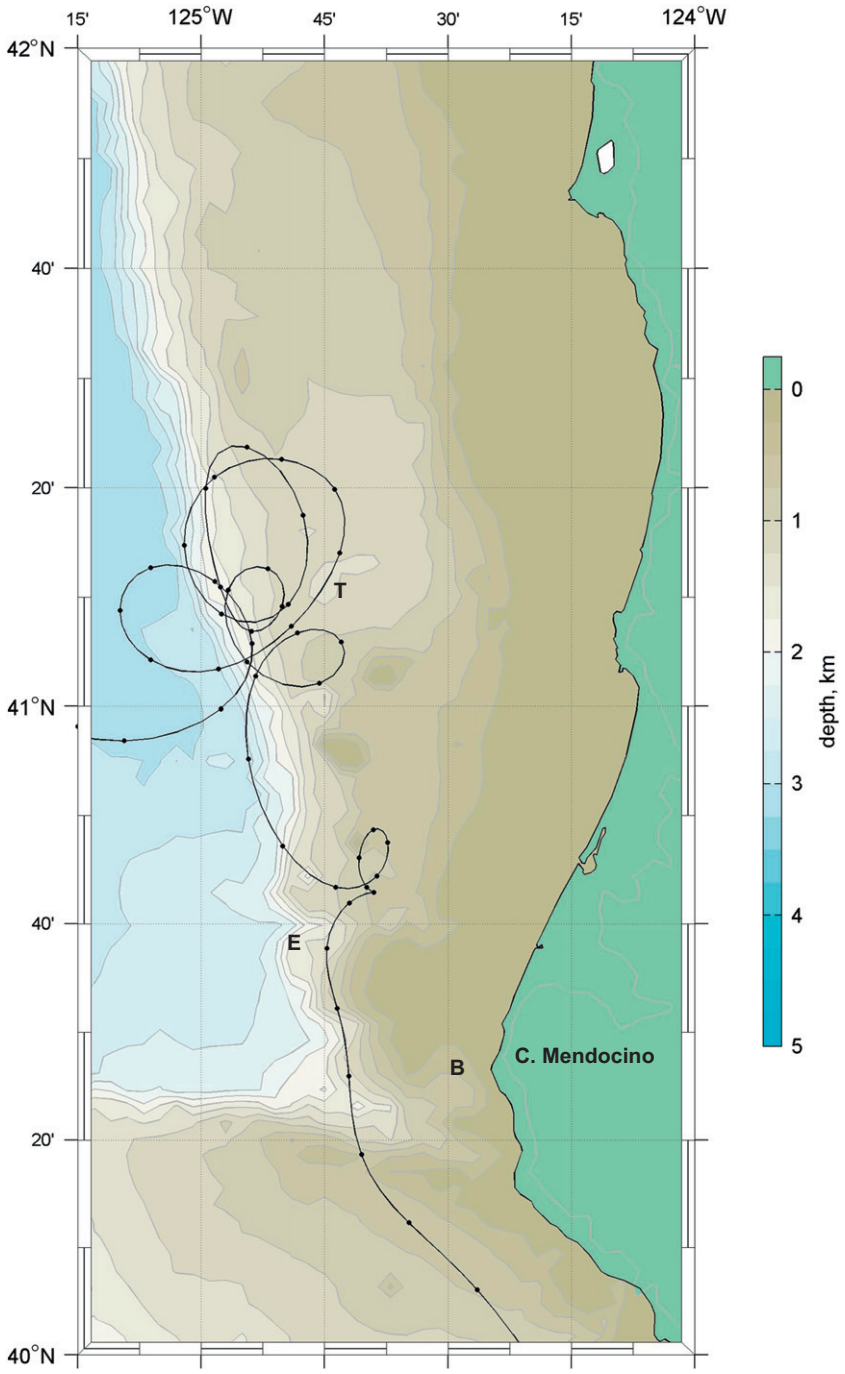

Fig. 6. Trajectory of Float 109 leaving the California Undercurrent to the north of Cape Mendocino and subsequently looping anticyclonically. The daily location is indicated by dots along the trajectory. Cape Mendocino is located at 40°27′N, 124°25′W and Trinidad Submarine Canyon ("*T*") is centered at 41°15′N, 124°40′W. The trajectory begins on 20 April 2005. "B" is Blunts Reef and "E" is Eel Submarine Canyon.

northward along the continental slope, moving offshore at 44°N and eventually looping. Float 87 passed Cape Mendocino a week later, moved offshore at 41.5°N, and did not loop. Float 8 crossed the westward path of Float 4 off Cape Mendocino five days after Float 8's passage and continued northward, apparently unaffected.

Based on the above, we estimated the time that it takes an eddy to form at Cape Mendocino to be five to ten days. To estimate the generation rate of anticyclonic loopers at Cape Mendocino, we modified the procedure described in Bower et al. (1997) by assuming that each year is the same. That is, if an anticyclonic looper is generated during one week in 1993, it will be generated during the same week in each of the following years. For weeks in which an anticyclonic looper is observed one year but is not observed by a float in a subsequent year, the annual generation rate would be one-half. A generation time of 5 to 10 days was used. This yielded a generation rate for Cape Mendocino of six anticyclonic eddies per year.

4.3. Anticyclonic characteristics

Histograms of kinematic characteristics of shallow, anticyclonic loopers are shown in Fig. 8. Probability distribution functions (PDFs) were determined for these histograms using methods appropriate for small samples. (See Appendix A.) Most loopers had diameters

Table 1
Kinematic characteristics of anticyclonic loopers. Italics indicate cuddies. Shaded row is deep looper.

Float ID	Start			Mean depth (dbar)	Mean temperature (°C)	Number of loops	Period (days)	Swirl speed (cm/s)	Diameter (km)	Translation speed (cm/s)	Direction (°T)
	Date mm/dd/year	Latitude (°N)	Longitude (°W)								
NPS#5	08/17/1993	42.17	125.35	148	7.8	2	7	19.6	37.7	0.8	134
NPS#6	01/03/1994	37.24	124.53	395	6.3	2	20	12.8	69.0	1.6	280
NPS#7	07/27/1993	37.18	125.04	341	6.9	5	7	19.8	38.1	2.9	283
NPS#8	10/17/1993	41.38	125.26	302	6.9	2	14	17.7	70.0	3.1	338
NPS#11	*11/23/1993*	*37.73*	*123.88*	*322*	*7.2*	*8*	*12*	*11.7*	*39.9*	*1.7*	*255*
NPS#13	11/26/1993	37.57	123.55	287	7.4	5	19	14.2	76.0	1.4	263
NPS#14	01/27/1994	37.92	124.55	–	7.3	4	21	9.5	54.2	1.1	296
NPS#19	06/30/1994	41.40	125.61	451	6.0	5	12	16.9	53.8	1.9	244
NPS#26	11/15/1994	39.00	124.48	320	7.6	4	11	10.1	30.1	4.0	288
NPS#28	10/28/1994	40.98	125.71	366	6.7	3	16	15.2	67.7	3.3	323
NPS#31	08/28/1994	38.00	125.27	372	7.0	5	25	21.0	141.6	1.7	250
NPS#33	12/09/1994	39.39	124.57	662	5.2	2	36	5.5	54.1	0.6	206
NPS#41	08/27/1996	37.55	124.10	735	4.9	3	64	11.6	203.4	0.9	255
NPS#43	04/16/1997	37.02	123.85	416	6.7	2	22	17.9	100.5	3.7	221
NPS#43	06/06/1997	36.20	127.67	422	6.7	3	63	11.1	192.9	1.9	256
NPS#48	02/01/1997	44.55	124.47	347	6.4	2	17	7.2	33.9	2.2	339
NPS#51	06/14/1997	36.58	127.53	360	7.0	3	93	9.5	241.4	1.1	249
NPS#57	11/16/1997	38.27	123.83	375	7.6	2	5	13.9	19.1	5.2	328
NPS#66	07/28/1999	37.33	123.38	405	6.8	2	13	9.9	35.4	1.1	112
NPS#66	08/30/1999	37.23	124.99	390	6.5	2	58	10.6	168.7	0.5	236
NPS#67	05/23/1999	40.64	125.77	390	5.8	5	5	20.0	25.3	7.2	256
NPS#67	06/18/1999	40.18	127.84	394	5.8	2	11	16.8	50.7	4.6	262
NPS#67	07/15/1999	40.45	129.34	401	5.9	7	13	15.4	55.3	0.2	241
NPS#69	08/23/1999	36.90	125.25	645	5.0	2	78	8.0	171.6	0.3	249
NPS#72	08/21/2000	40.77	126.76	738	4.5	2	48	7.5	98.9	2.8	249
NPS#73	*12/13/1999*	*36.14*	*123.72*	*315*	*7.9*	*30*	*14*	*19.4*	*76.0*	*2.1*	*256*
NPS#74	*11/29/1999*	*36.55*	*122.82*	*1545*	*2.7*	*31*	*9*	*9.6*	*24.6*	*1.1*	*289*
NPS#75	06/29/2000	38.57	126.61	118	10.2	2	25	15.2	103.4	2.4	217
NPS#83	*10/22/2001*	*42.21*	*126.52*	*232*	*8.0*	*9*	*8*	*26.3*	*54.3*	*2.2*	*290*
NPS#85	06/09/2001	42.99	127.79	131	8.6	4	11	16.2	49.0	0.7	264
NPS#88	12/19/2001	43.94	126.67	471	5.4	6	19	9.2	47.2	1.3	280
NPS#89	08/15/2001	40.66	124.83	323	6.7	5	5	13.6	17.3	2.3	333
NPS#89	09/26/2001	42.16	125.55	347	6.8	3	4	17.4	20.8	3.4	43
NPS#90	01/24/2002	38.54	125.93	309	7.2	2	28	14.3	108.9	2.2	320
NPS#90	*11/05/2003*	*47.22*	*125.34*	*319*	*6.8*	*30*	*4*	*18.2*	*20.8*	*1.6*	*322*
NPS#91	08/22/2002	40.60	129.50	349	6.7	3	29	9.3	74.9	3.2	279
NPS#98	*04/13/2004*	*37.05*	*124.42*	*344*	*7.6*	*13*	*23*	*11.4*	*73.5*	*3.1*	*237*
NPS#98	02/04/2006	32.87	132.53	378	7.8	2	39	9.2	97.0	2.4	259
NPS#102	12/17/2003	47.13	125.18	339	6.7	3	10	13.1	35.2	4.6	3
NPS#104	*12/02/2002*	*37.13*	*123.01*	*317*	*7.6*	*19*	*15*	*14.0*	*59.3*	*1.4*	*247*
NPS#105	*07/23/2003*	*34.66*	*121.74*	*321*	*7.8*	*8*	*20*	*20.1*	*111.8*	*1.9*	*286*
NPS#106	*07/23/2003*	*34.73*	*121.56*	*329*	*8.0*	*30*	*16*	*20.4*	*93.2*	*1.8*	*246*
NPS#107	*08/26/2005*	*41.64*	*125.07*	*348*	*7.3*	*72*	*6*	*16.5*	*28.1*	*2.0*	*274*
NPS#109	*05/13/2005*	*41.08*	*124.89*	*364*	*7.4*	*65*	*8*	*20.9*	*48.2*	*3.2*	*245*
NPS#111	11/16/2006	36.39	129.95	351	7.2	2	58	8.1	130.4	0.6	153
NPS#111	04/25/2007	33.94	131.79	395	7.6	2	53	8.6	124.8	0.7	117
NPS#115	02/25/2008	39.61	126.41	291	7.2	2	36	15.9	157.9	0.5	185
NPS#115	08/05/2008	43.16	125.09	288	7.1	2	8	24.2	50.2	4.9	300

between 25 and 100 km, and 11 rotated in loops of larger diameter (Fig. 8A). The largest number of anticyclonic loopers had 55–70 km diameter with a median value of 54.8 km. The PDF for loop diameters was close to a Weibull distribution. Loopers with diameters which exceeded 150 km (Floats 41, 43, 51, 66, 69, 115) moved along very complicated trajectories with only 2–3 consecutive anticyclonic loops.

The period of the float rotation varied between 4 (Floats 89, 90) and 93 (Float 51) days and the median value was 15.5 days (Fig. 8B). The two most populated groups rotated with periods between 5 and 15 days, and 15 and 25 days (Fig. 8B). Note that the diameters of the loops in the former group did not exceed 80 km, and the latter group contained loops with diameters between 30 and 150 km (Table 1). There were six loopers that had a much longer period, 45–65 days (the PDF includes these as a second mode). While the larger diameter loopers usually had a longer period, it is difficult to conclude if the relationship was linear based upon data in Table 1.

The swirl, or rotational, speed of the loopers was distributed almost uniformly between 7 and 21 cm/s, with a slight maximum at 17 cm/s and a median value of ~15 cm/s (Fig. 8C). One looper (Float 83) had a higher swirl speed, about 26 cm/s. Note that most loopers with swirl speeds of ~20 cm/s (Floats 5, 7, 31, 67, 73, 90, 105, 106, 109) made more than 10 consecutive loops (Table 1). The PDF for swirl speed was close to uniform and could not be determined for these data.

Translation speeds and directions are shown in Fig. 8D and E, respectively. The peak was at 2 cm/s and the median value was 1.9 cm/s (Fig. 8D). This corresponded to previous estimates of westward transport speed in this region (Ivanov et al., 2008). The one outlier, 7.2 cm/s, was Float 67. The trajectory of Float 67 was unusual, as it changed rotational patterns three times. The distribution of the mean direction (direction is measured clockwise from north) of looper motion (Fig. 8E) indicated that anticyclonic loopers usually moved normal to the coastline. The median value was 256°, similar to the value of 261° obtained

Table 2
Kinematic characteristics of cyclonic loopers. Italics indicate long-lived loopers. Shaded row is deep looper.

Float ID	Start			Mean depth (dbar)	Mean temperature (°C)	Number of loops	Period (days)	Swirl speed (cm/s)	Diameter (km)	Translation speed (cm/s)	Direction (°T)
	Date mm/dd/year	Latitude (°N)	Longitude (°W)								
NPS#29	10/24/1995	35.98	121.74	395	6.78	2	10	5.4	14.7	2.1	280
NPS#32	10/04/1995	37.08	128.81	293	7.51	3	65	7.6	135.2	2.0	276
NPS#53	11/29/1997	38.80	125.43	290	6.64	2	16	8.5	36.2	2.0	267
NPS#57	02/17/1998	38.88	126.29	321	6.79	2	9	12.8	31.7	2.6	302
NPS#66	*10/27/1998*	*36.01*	*121.83*	*404*	*6.25*	*12*	*19*	*6.2*	*32.1*	*0.8*	*224*
NPS#75	10/31/2000	36.58	129.58	77	11.24	2	26	14.5	103.8	1.6	220
NPS#79	*12/21/2000*	*37.17*	*123.34*	*1167*	*3.51*	*12*	*16*	*8.8*	*37.7*	*1.6*	*270*
NPS#82	03/03/2001	41.63	127.90	205	7.54	3	55	6.3	95.2	1.2	298
NPS#83	09/15/2000	36.21	122.26	262	7.51	2	113	5.7	80.1	1.0	184
NPS#85	10/05/2001	41.84	127.95	232	8.00	6	46	13.8	176.5	1.6	258
NPS#88	06/19/2003	42.95	125.92	334	5.91	2	20	10.2	56.4	4.1	314
NPS#92	01/23/2004	39.21	127.97	286	6.06	2	15	6.7	28.1	2.3	298
NPS#92	04/08/2003	40.42	129.41	290	6.37	2	51	5.2	72.4	1.3	254
NPS#92	12/28/2001	37.60	124.34	291	7.13	2	16	6.6	29.2	2.5	296
NPS#108	*12/06/2006*	*36.30*	*124.57*	*339*	*7.09*	*73*	*5*	*10.9*	*15.2*	*3.4*	*290*
NPS#111	*10/27/2005*	*36.52*	*122.61*	*313*	*7.19*	*16*	*12*	*12.2*	*38.7*	*1.7*	*220*
NPS#112	*10/29/2005*	*36.62*	*122.59*	*334*	*7.24*	*78*	*5*	*10.1*	*13.9*	*1.0*	*238*
NPS#113	10/11/2009	36.54	130.56	276	7.64	2	38	14.3	144.7	0.6	343

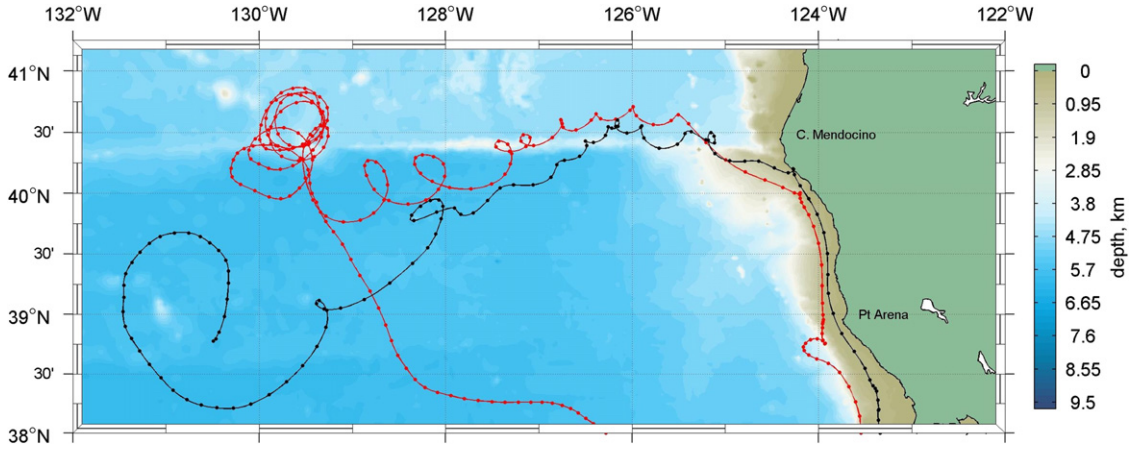

Fig. 7. Trajectories for Float 4 (black) and Float 67 (red) leaving the continental margin at Cape Mendocino and subsequently looping anticyclonically. The daily location is indicated by dots along the trajectory. Cape Mendocino is located at 40°27′N, 124°25′W. The trajectories shown here begin to the south of Pt. Arena near 38°N on September 8, 1993 (April 9, 1999) for Float 4 (Float 67). (For interpretation of the references to color in this figure legend, the reader is referred to the web version of this article.)

for trajectories of eddies computed from altimeter data (Schlax and Chelton, 2008). The exception here corresponded to five loopers which moved alongshore or slightly deviated from the alongshore direction. Only one of these northward moving loopers occurred south of Cape Blanco, and all were observed between mid October and early February. The only northward moving cuddy, Float 90, had small diameter loops, 20.8 km (Table 1). Looping motion originated at the entrance to Quinault Submarine Canyon on November 5, 2003, when the seasonal circulation was likely representative of subpolar conditions with surface Eastern Boundary currents directed poleward (Hickey, 1989).

Long-lived (> 70 days, 8 or more consecutive loops) anticyclonic loopers, i.e., cuddies, are identified in Fig. 8 as a subset of the looper histograms. A large gap, about six years (November 1993 to December 1999), existed between observations of long-lived loopers (Table 1). Some of this gap can be explained by the use of relatively short 120-day missions prior to 1997: given the mean eddy capture time of 100 days, only Float 11 looped longer than 70 days. Few floats were launched in 1997 and 1998, and some of these floats failed. Beginning in April 1998, a new design of float closure was adopted that eliminated leaking between the end cap and glass tube. The later missions were 825 days, which made eddy encounter and looping probable. But it is possible that the number or location region of eddies could change from year to year.

Compared to the total population of anticyclonic loopers, cuddies typically had smaller diameters and shorter periods. The cuddies also had higher swirl speeds than the total population and thus larger vorticity magnitude. The direction of translation for cuddies was from 250° to 350°. The mean speed and vector mean direction for the translation of cuddies were 2.1 cm/s and 259°, respectively.

The translation paths for the long-lived floats are shown in Fig. 9. In addition to westward movement, the cuddies were displaced northward by the CUC as they left the continental slope. On leaving the CUC, Floats 98, 106 and 109 were displaced southward by the inshore edge of the California Current. While the cuddies mostly moved steadily to the west, Float 106 turned eastward at about 32°N, 130°W on September 23, 2004.

4.4. Cuddy water properties

Cuddy water properties resemble those of California Undercurrent waters. For the eddies described here, only when (and because)

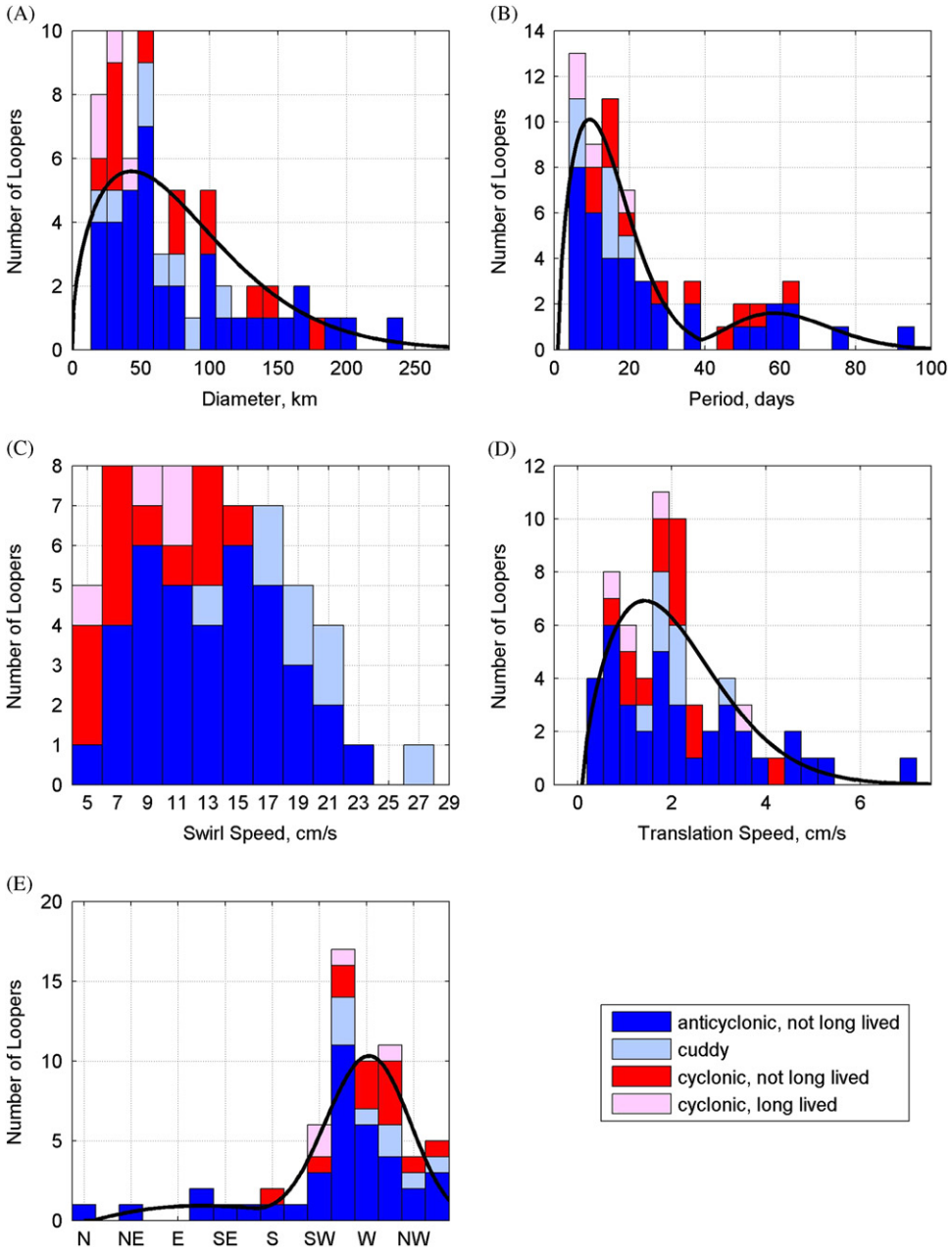

Fig. 8. Distribution of mean kinematic characteristics for anticyclonically [blue] (cyclonically [red]) looping trajectories. Light blue (light red) indicates long-lived (> 70 days and at least 8 consecutive loops) anticyclonic (cyclonic) loopers. Probability distribution functions (black lines) have been fitted to anticyclonic looper data, as described in Appendix A. (A) Diameter, km. (B) Period, days. (C) Swirl speed, cm/s. (D) Translation speed, cm/s. (E) Translation direction, degrees True. (For interpretation of the references to color in this figure legend, the reader is referred to the web version of this article.)

Floats 105 and 106 were serendipitously launched into a cuddy did hydrographic measurements get made of the structure of a portion of an eddy core. A chart of the ship track and velocity measurements at 300 dbar is shown in Fig. 10 (upper). The *R/V Point Sur* proceeded inshore along *Cal*ifornia *C*ooperative *F*isheries *I*nvestigations (CalCOFI) Line 77 and hove to for 1000 m CTD casts every 10 n. mile (18.5 km). Float 105 was launched at CalCOFI station 77-62.5 at 23:58 UTC on 23 July 2003; two hours later, Float 106 was launched at CalCOFI station 77-60. Acoustic Doppler Current Profiler measurements showed that currents at 300 dbar near these stations were directed east-northeastward or eastward at 20 cm/s, reflecting the initial eastward displacement of both floats. Note that the time difference between two successive points on the float trajectory (one day) was greater than that spent by the ship along CalCOFI Line 77 (18 h).

Hydrographic sections of density anomaly and spiciness for Line 77 are shown in Fig. 10 (lower) along with the location of Floats 105 and 106. (Spiciness is a conservative property used to characterize temperature–salinity characteristics; changes in spiciness are poorly correlated with density [Flament, 2002]). The sections show the existence of the Undercurrent next to the upper slope: isopycnals sloped downward toward the coast below 100 m, and waters above 300 m have spice > 0.05 kg/m^3 (characteristic of their low latitude origin as subsurface subtropical waters). Waters of similar characteristics were observed at the location of the floats (about 100 km from the coast) in an isopycnal trough. These two similar waters were separated by a shoaling of isopycnals (about 50 dbar to the west for the 26.8 kg/m^3 isopycnal) and a decrease in spice to ~ 0 kg/m^3, the latter associated with California Current waters.

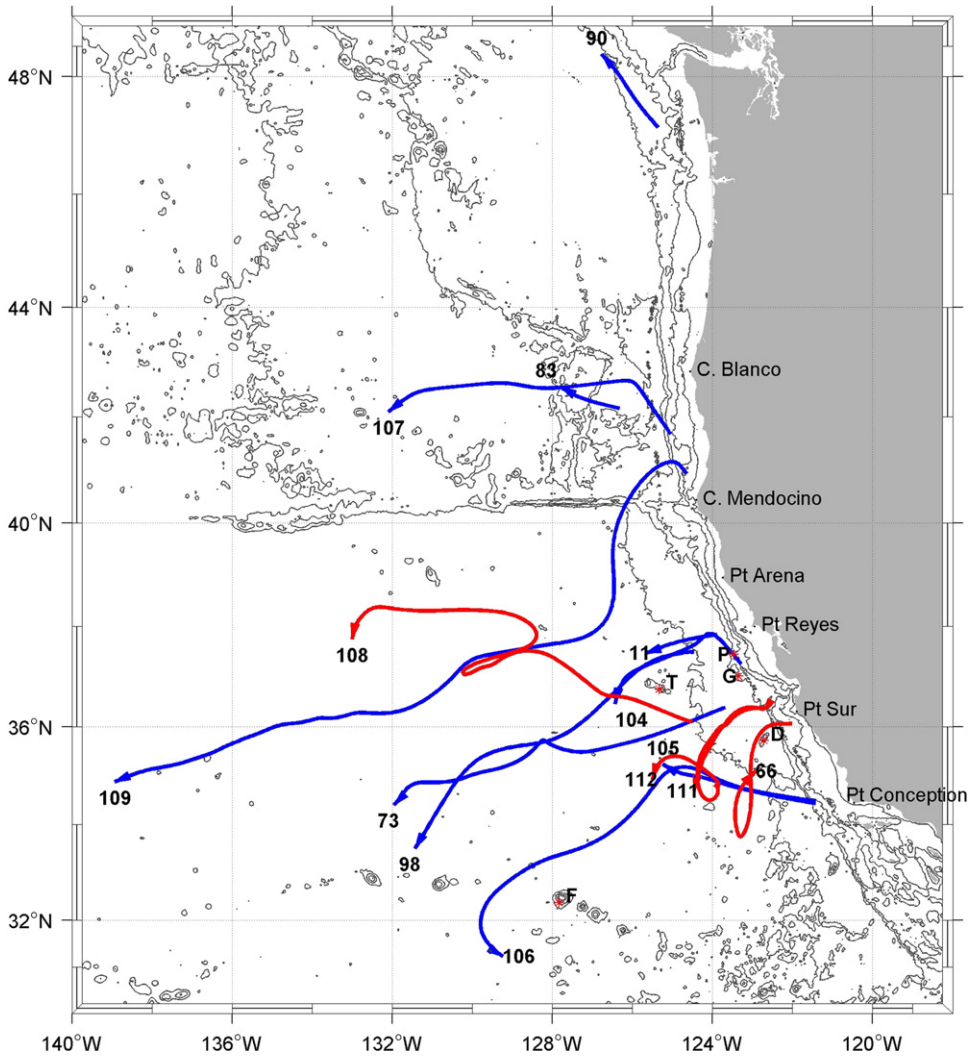

Fig. 9. Translation of long-lived looping floats. (The looping motion has been removed.) Observations span the interval from November 1992 to December 2007. Blue (red) indicates anticyclonic (cyclonic) looping motion. Numbers identify individual floats. Isobaths are 200, 1000, 2000, 3000, and 4000 m. Seamounts include Fieberling (F), Taney (T), Pioneer (P), Guide (G) and Davidson (D).

Two other features of the cuddy structure should be noted. The trough in the density field moved offshore (west and south) with depth, consistent with the observed westward translation of the cuddy. Second, in the upper 100 m of the cuddy, the slope of the isopycnals reversed, forming a dome-like cap. This structure is similar to that seen at the coast, and reflects vertical shear above the deeper core of flow. It also means that a temperature minimum at the sea surface marked the cuddy location.

The center of this cuddy was likely displaced by at least 50 km south of the location of the hydrographic data as indicated by the float paths around the cuddy during the first 12 days of their missions. Hence, the aforementioned hydrographic data likely represented water characteristics in the outer region of the eddy.

Profiles of density, spice, salinity and dissolved oxygen for CUC waters inside and outside the cuddy are shown in Fig. 11. Cuddy waters resemble those found in the CUC: along isobars between 100 and 500 dbar, cuddy waters are less dense, saltier, spicier and lower in oxygen than those outside the eddy. Largest differences occurred between 100 and 225 dbar and water density 26.5 kg/m^3 and were 1.3 °C, ΔS=0.22, 0.34 kg/m^3, and 82 μmol/kg for temperature, salinity, spiciness and dissolved oxygen, respectively.

The observed water properties of the July 2003 cuddy can be compared with those for a July 1985 section through the center of a 100 km diameter cuddy located at 33°N, 123°W (Simpson and Lynn, 1990). They observed cuddy core properties between 100 and 500 dbar with maximum anomalies of 1 kg/m^3 spiciness and 400 μmol/kg dissolved oxygen at a depth of 250 dbar, about four times those observed, between the outer core and ambient waters of the January 2003 cuddy. A cuddy observed north of Oahu (22.75°N, 158°W) in January 2001 by Lukas and Santiago-Mandujano (2001) had maximum anomalies of ΔS=0.6 and 180 μmol/kg dissolved oxygen near 400 m depth, although they are uncertain that these anomalies were at the center of the cuddy. These observations confirm that core waters of cuddies consist of California Undercurrent waters which are most easily identified between 100 and 250 dbar by large horizontal gradients between the core waters and surrounding California Current waters.

4.5. Cyclonic eddy characteristics

Kinematic characteristics for 15 shallow cyclonic loopers are tabulated in Table 2 and also shown in Fig. 8. Compared to the population of anticyclonic loopers, the cyclonic looper

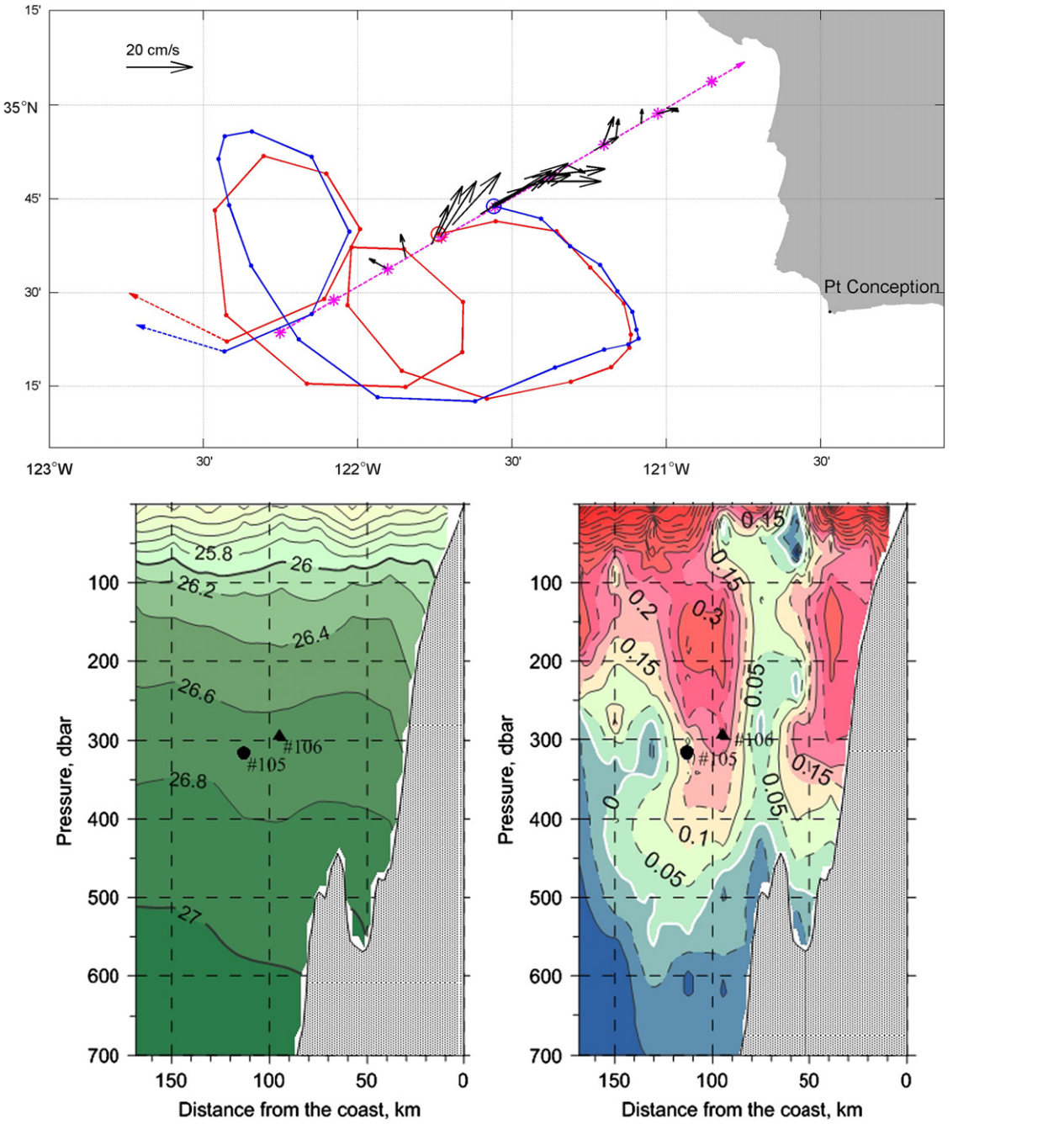

Fig. 10. Hydrographic structure associated with anticyclonic looping motion of Floats 105 and 106. [Upper] Chart showing ship's track (magenta) on July 23, 2003, hydrographic stations (magenta asterisks), launch locations and subsequent trajectory of Floats 105 (red circle and line) and 106 (blue circle and line), and vessel mounted acoustic Doppler currents (black arrows) at 300 m. Dots along trajectories are one day apart. The ship track shown took a total of 18 h. [Lower Left] Density anomaly, kg/m^3. Contour interval is 0.2 kg/m^3. [Lower Right] Spice, kg/m^3. Contour interval is 0.05 kg/m^3.

distributions showed somewhat smaller diameters (principal mode was 25 vs. 50 km) and longer periods (20 vs. 10 days principle mode). (One cyclonic looper, Float 83, had a longer period than any other looper, 113 days.) As a consequence, the swirl speeds were much smaller (7 vs. 17 cm/s). The translation of the cyclonic loopers was directed somewhat northward compared to that of the anticyclonic loopers (300° vs. 250°), but the translation speed was similar (1.8 vs. 2 cm/s). Note that observations from altimetry show that cyclones tend to deflect poleward and anticyclones tend to deflect equatorward (Chelton et al., 2011).

Four long-lived cyclonic loopers (Floats 66, 108, 111, 112) were identified. Their smoothed trajectories are shown in Fig. 9. These long-lived cyclonic loopers generally moved to the west. But unlike the anticyclonic loopers, their smoothed trajectories usually included superimposed large cyclonic (Floats 108 and 112) and anticyclonic (Float 66) loops. Eastward movement in these loops occurred during spring or summer: Float 66 from April 15 to June 30, 1999; Float 112 from May 17 to August 11, 2006; and Float 108 from July 10 to August 12, 2006. Since similar seasonal features do not appear in the anticyclonic eddies, it is difficult to ascribe the easterly flows to a reversal of the background currents, e.g., seasonal spin up of the Southern California Eddy (Bray et al.,1999). Nonlinear Rossby wave packets could be responsible for these eastward motions (Ivanov et al., 2010).

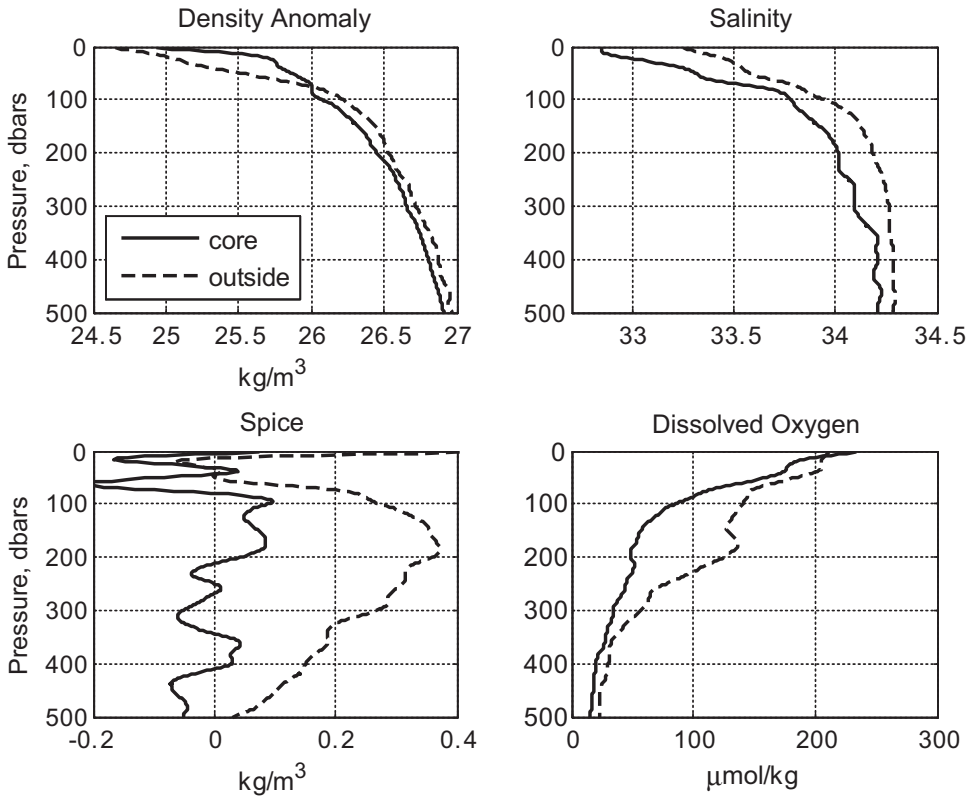

Fig. 11. Profiles of eddy properties measured during the launch of Floats 105 and 106, 23–24 July, 2003. [Upper left] Density anomaly, kg/m^3. [Upper right] Salinity. [Lower left] Spice, kg/m^3. [Lower right] Dissolved oxygen, µmol/kg.

4.6. Termination of looping motion

Eight in situ terminations of long-lived looping were observed. Terminations were either smooth or abrupt. In the case of a smooth transition, the float would continue flowing in the same direction, ceasing its rotation around the loop. For an abrupt transition, the float would change its direction when leaving the loop and changes in the temperature and pressure relationship would occur, the latter indicating a change in the stratification of the ambient waters (Boebel et al., 1995).

Five transitions were smooth (including both deep floats) and three transitions were abrupt. For cuddies, the four observed transitions took place when the float was moving north or northeast, while among the four cyclonic translations, three were southward and one was northward.

An example of abrupt termination for cuddy looping (Float 105) is shown in Fig. 12. After looping began on July 23, 2003, the diameter of the looping motion first decreased to 50 km and maximum temperatures, 8.2 °C, were observed during the third loop. The diameter of looping subsequently increased and the temperature cooled at a rate of 0.0034 °C per day. The last loop had a diameter of 140 km, and as Float 105 rotated toward the southeast on January 12, 2004, it suddenly steadied on a southward course while the temperature dropped from 7.6 °C to 6.9 °C during the next two days. The float trajectory shows a subsequent cyclonic loop. The character of the temperature vs. pressure relationship changed after this transition from anticyclonic to cyclonic looping, and the temperature recorded by the float began to increase at a rate of 0.0064 °C per day.

Abrupt termination of long-lived cyclonic looping (Float 111) is shown in Fig. 13. Float 111 began cyclonic looping on October 27, 2005, with ambient temperature of 7.5 °C. During the period of cyclonic looping, the temperature decreased at a rate of 0.0018 °C per day. When circuiting the northeastern segment of the cyclonic loop located at 35.5°N, 124°W, minimum temperatures of 6.75 °C occurred. The pressure vs. temperature relationship shifted about −0.3 °C during the period of cyclonic looping. On July 18, 2006, Float 111 abruptly ceased cyclonic looping and changed course from southward to northwestward. A month later a minimum temperature of 6.72 °C was recorded, and Float 111 subsequently warmed at a rate of 0.0082 °C per day. At this time, the pressure vs. temperature relationship had shifted by −0.2 °C and the slope increased, the latter indicative of a change in stratification.

Both cyclonic and anticyclonic eddies showed distinct core properties that change slowly with time, most likely due to the lateral entrainment of ambient waters (Simpson and Lynn, 1990). With time, the floats seemed to move away from the eddy center where they were subject to detrainment from the eddy by ambient flow or other mesoscale features.

4.7. Floats that looped both cyclonically and anticyclonically.

The trajectories for the seven floats that were entrained in both cyclonic and anticyclonic eddies are shown in Fig. 14. After looping cyclonically, Floats 66 and 83 moved poleward in the CUC. Float 66 (83) took 267 km (876 km) and 46 days (177 days) to complete this poleward transit and loop anticyclonically. Float 66 (83) swirl speeds for cyclonic looping were 6.2 cm/s (5.7 cm/s) and 9.9 cm/s (26.3 cm/s) for anticyclonic looping. Given the length of time and distance between the looping events and the mismatch of swirl speeds, the trajectory of floats 66 and 83 is unlikely to represent an interacting counter-rotating eddy pair. Similar arguments (long transition distance, period and mismatch in swirl speeds) can be made for floats 85, 88 and 111.

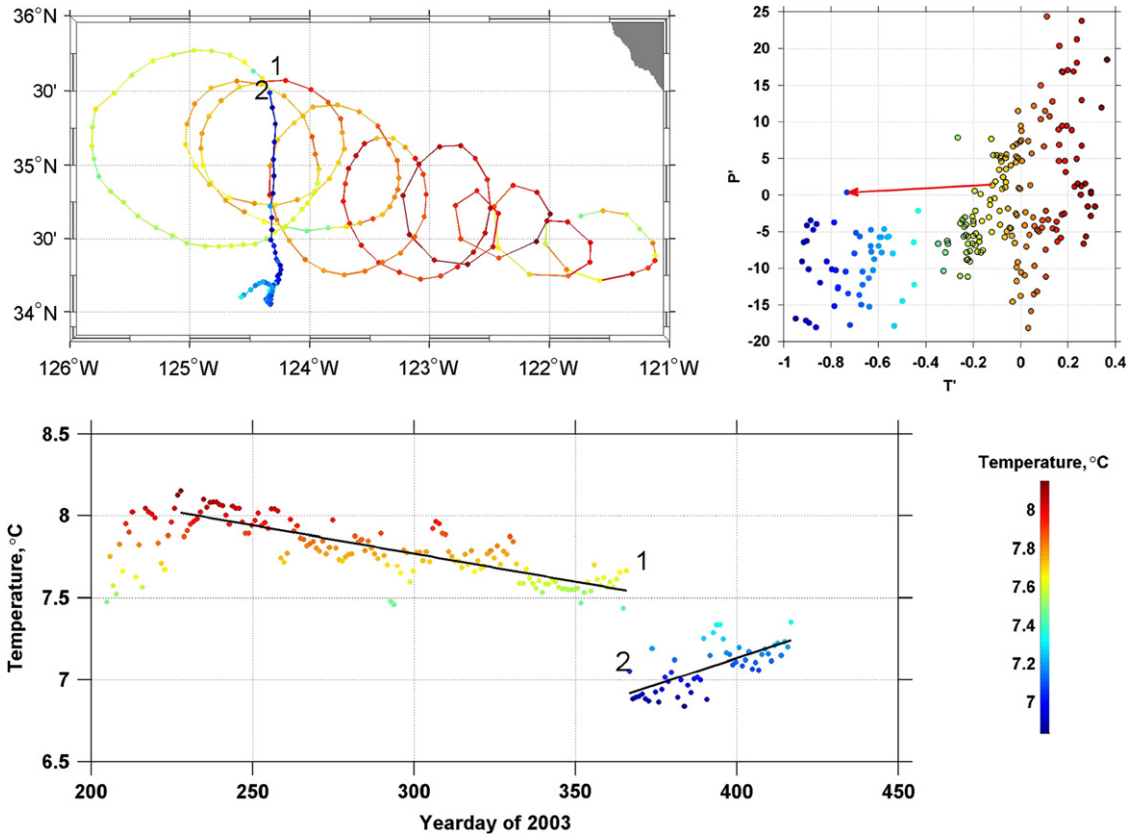

Fig. 12. Abrupt termination of long-lived anticyclonic looping (Float 105). Data are shown every 12 h. The temperatures of the data points are given by the temperature scale in the lower right hand corner. Termination of looping is indicated by "1" and the subsequent temperature minimum by "2." [Upper left]. Trajectory for Float 105. [Upper right]. Pressure (dbar) vs. temperature changes relative to the mean temperature (7.8 °C) and mean pressure (322 dbar) of the looping. The red arrow shows the transition from the termination of looping to the subsequent temperature minimum. [Lower]. Temperature vs. 2003 yearday.

Only one float (75) was observed to transition directly from anticyclonic looping to cyclonic looping (Fig. 14). On June 29, 2000, Float 75 initially encountered two anticyclonic loops of 103 km diameter near 38°N, 127°W. After completing these two loops, Float 75 continued around another anticyclonic loop about twice the size, moved 175 km to the southwest, and looped twice cyclonically beginning on October 31, 2000. The swirl speeds for the loops were in good agreement, 15.2 cm/s for anticyclonic loops (Table 1) and 14.5 cm/s for cyclonic loops (Table 2). The mean temperature (mean pressure) for the anticyclonic motion was 10.2 °C (118 dbar) and 11.24 °C (77 dbar) for cyclonic motion and implies an increase in salinity of about 0.4 (calculated following Boebel et al., 1995). If the anticyclonic and cyclonic motions were coupled, then their propagation speed was 2.2 km/day to the southeast.

The final incidence of sequential counter rotation shown in Fig. 14 is Float 57. It initially loops cyclonically while moving poleward in the Undercurrent near Point Arena on November 16, 1997. Note that, although Table 2 identified only two loops, the epicycloidal character of the poleward transit continued to near Cape Mendocino. The float subsequently moved inshore at Cape Mendocino, thence south to Point Arena, where it moved offshore to about 126°W and began anticyclonic looping on February 17, 1998. The swirl speeds for the cyclonic loops, 12.8 cm/s, increased to 13.9 cm/s for the anticyclonic loops. Despite the similar swirl speeds, the 8.5 months transit between looping argues against interaction of counter rotating eddies.

In summary, the RAFOS floats did not seem to be readily exchanged between cyclonic and anticyclonic loopers. The one exception to this behavior was Float 75 which was quite shallow, about 100 dbars. Based on the structure of cuddies described above and by Simpson and Lynn (1990), Float 75 was above the eddy core and likely influenced by near surface processes which would aid in its detrainment and exchange.

4.8. Deep loopers

Both deep loopers occurred to the west of Monterey Bay, one cyclonic (Float 79) at a depth of 1167 dbar and the other anticyclonic (Float 74) at a depth of 1545 dbar (Fig. 15). The anticyclonic looper began in late November 1999, about 13 months before the cyclonic looper in December 2000. Both loopers had an explicit topographic nature due to their generation near complicated bathymetry offshore from Monterey Bay. A small epicycloidal loop occurred prior to anticyclonic looping by Float 74. The pre-looping trajectory of the cyclonic float (79) traced two sinusoids of seven-day duration and 7-km amplitude as the float moved westward between Pioneer (820-m summit) and Guide (1682-m summit) Seamounts. Both deep loopers were long-lived, the anticyclonic (cyclonic) looper for 279 (192) days, and moved westward, ending near Taney Seamounts. A complete description of the float trajectories and temperature and pressure measurements can be found in Zamora (2009).

The kinematic characteristics of the anticyclonic looper (Table 1) compared well with its long-lived shallow counterparts (Fig. 8) except for the slow translation speed, 1.1 cm/s compared to 1.4 cm/s for the slowest shallow looper (Float 104). All the kinematic characteristics for the cyclonic looper fell within the range of those for long-lived shallow cyclonic loopers (Table 2, Fig. 8). At the end of anticyclonic looping, the pressure–

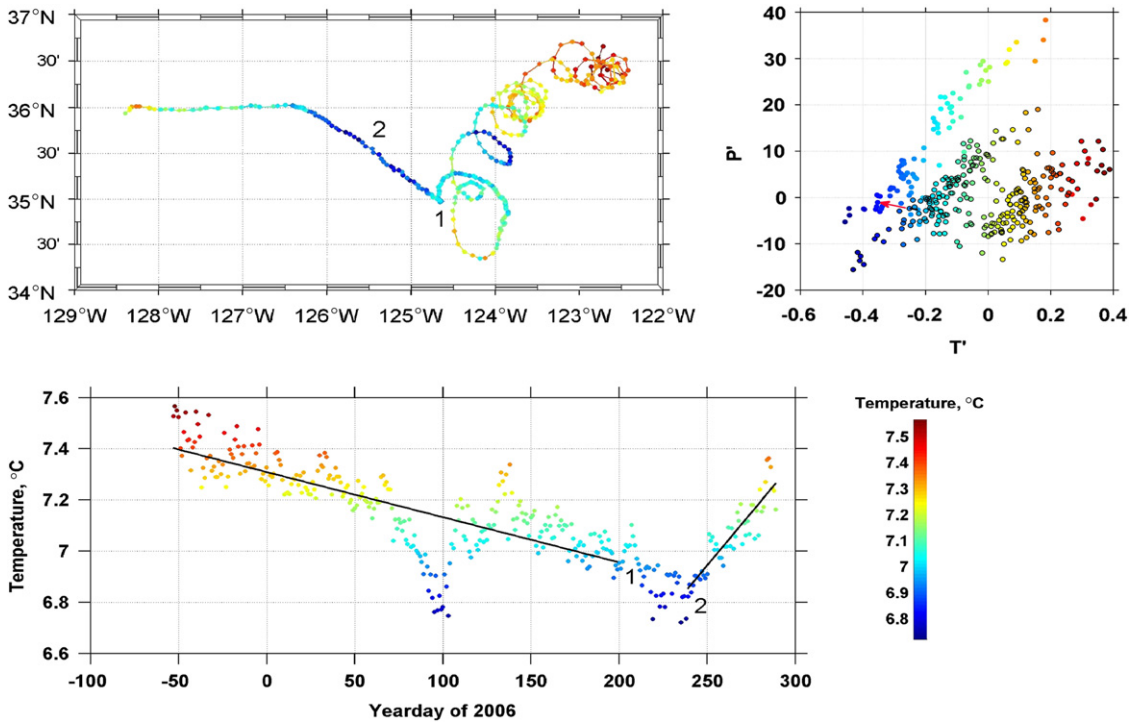

Fig. 13. Abrupt termination of long-lived cyclonic looping (Float 111). Data are shown every 12 h. The temperatures of the data points are given by the temperature scale in the lower right hand corner. Termination of looping is indicated by "1" and the subsequent temperature minimum by "2." [Upper left]. Trajectory for Float 111. [Upper right]. Pressure (dbar) vs. temperature changes relative to the mean temperature (7.2 °C) and mean pressure (313 dbar) of the looping. The red arrow shows the transition from the termination of looping to the subsequent temperature minimum. [Lower]. Temperature vs. 2006 yearday.

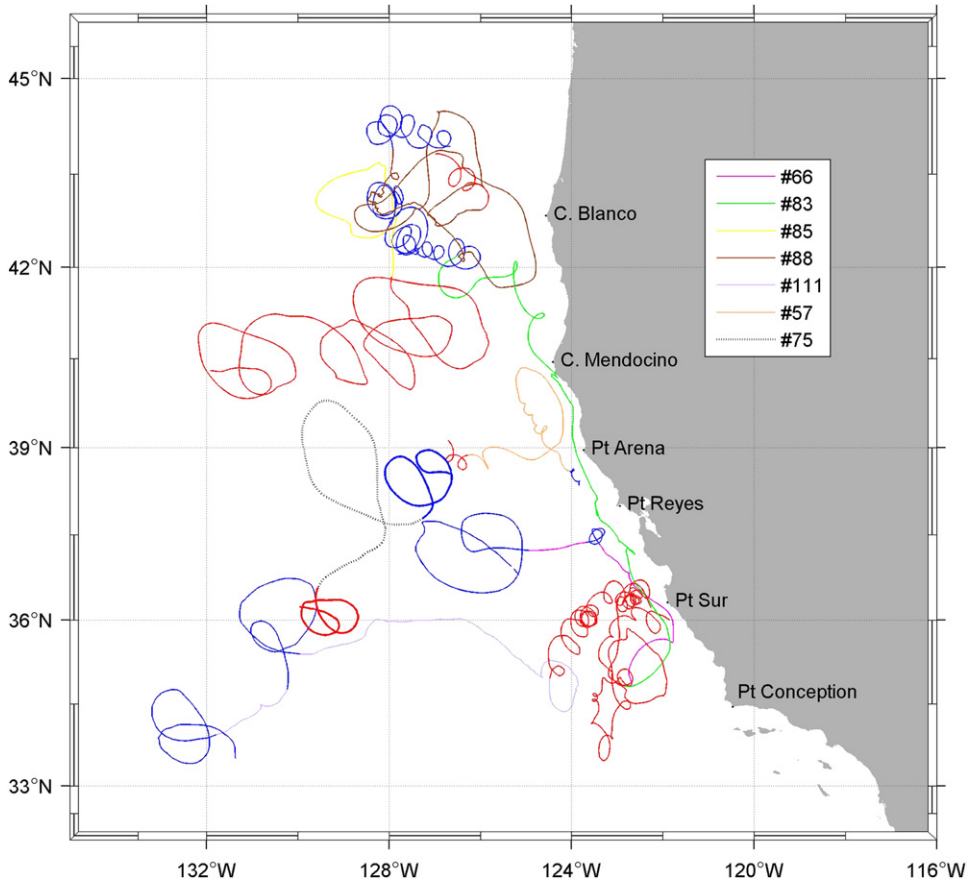

Fig. 14. Trajectories of floats that looped in both directions. Individual trajectories are as indicated in the legend, except that cyclonic looping is red and anticyclonic looping is blue.

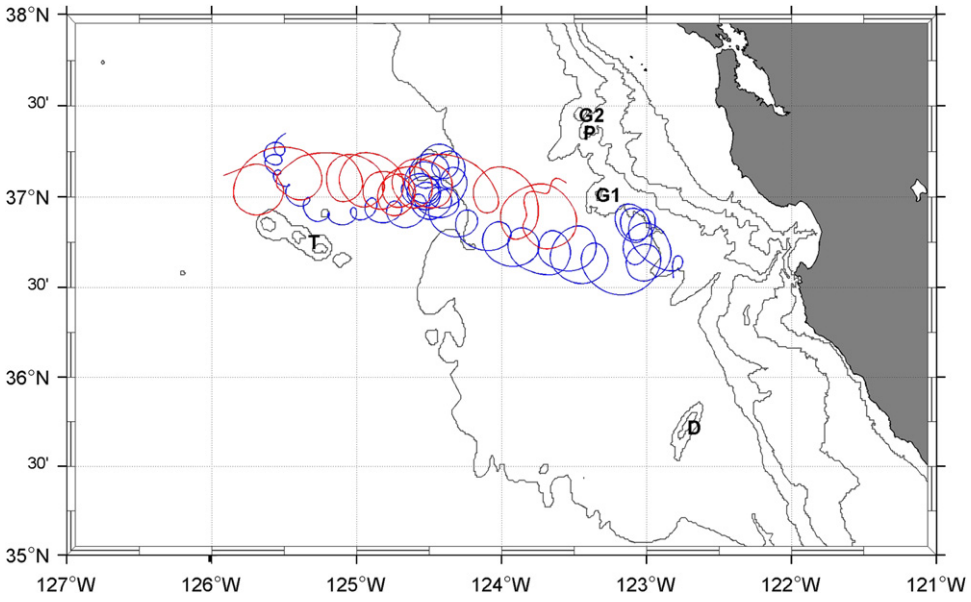

Fig. 15. Deep loopers. Blue (red) indicates anticyclonic (cyclonic) motion at a depth of 1545 (1167) m for Float 74 (79). The trajectories are about one year apart. The anticyclonic (cyclonic) looping trajectory began on 29 November 1999 (21 December 2000) and included 31 (12) loops of 9 (16) day period and 24.6 (38) km diameter. Pre- and post-looping epicycloidal motion is shown for the anticyclonic looper and pre-looping sinusoidal motion for the cyclonic looper. Isobaths are 200, 1000, 2000, 3000, and 4000 m. From west to east, seamounts are Taney (T), Gumdrop (G2), Pioneer (P), Guide (G1), and Davidson (D).

temperature relationship indicated that the ambient water properties had changed; so this looper represented long-lived eddy motion. The pressure sensor on the deep cyclonic looper did not appear to have functioned properly. (At one point during the looping motion, the pressure sensor indicated that the float was at 1450 dbars and the measured temperature was 3.5 °C, about 0.6 °C warmer than temperatures measured by historical CTDs at this depth near this location.)

Looping terminated for both loopers when they were in the vicinity of the Taney Seamounts. The shallowest depth in the seamount chain is 2800 m, well below the depth of the looper. The cyclonic looping ended about a half cycle after the float passed just north of the tallest submarine volcano in the chain. The looping motion for the anticyclonic float changed from circular to epicycloidal at 125.5°W and continued northwestward along the northern edge of the seamount. When the looper was well clear of the seamount chain, anticyclonic looping motion stopped.

5. Summary

Isobaric RAFOS floats launched at 300 m over the continental shelf along the Central California coast were usually transported poleward in the California Undercurrent. These floats spent about 26% of their time looping, with a two to one preference for anticyclonic vs. cyclonic rotation. Cuddies were stable and robust and transported fluid considerably farther offshore than the 400-km distance observed previously (Chereskin et al., 2000; Garfield et al., 1999). One cuddy (109) moved southwestward 1650 km over a period of 520 days (similar to observed westward translation distances by meddies in the Atlantic). Temperature changes associated with floats leaving eddies indicated warm water cores. The observations of cuddies confirm properties of long-lived sea surface height anomalies described by Chelton et al. (2011). These cuddies are important because they provide an efficient mechanism to move near surface upwelled coastal waters and associated subsurface coastal waters of Equatorial origin into the interior of the North Pacific Subtropical gyre.

Anticyclonic eddies were observed to form near Cape Mendocino due to the interaction of the undercurrent with bottom topography. In some cases, the eddy was formed inshore; but in others the eddy was advected westward and formation delayed due to the strength of the offshore flow. Eddies formed by these mechanisms likely originated on the inshore side of the horizontal velocity maximum of the CUC. About half the time, looper initiation was preceded by epicycloidal motion. (Pierce et al., 2000, documented flow conditions around Cape Blanco using shipboard ADCP observations from July to August 1995 and observed an anticyclonic eddy forming on the offshore side of the CUC.) Looping RAFOS floats also showed anticyclonic looping behavior beginning offshore and not associated with the inshore track of the float. While it is tempting to suggest that this offshore looping may be caused by baroclinic instability, it could also represent a float becoming entrained in a long-lived eddy which was formed inshore and had propagated offshore. Both processes, baroclinic instability and topographic drag, should be incorporated into high resolution numerical ocean models to accurately represent long-lived anticyclonic eddies and associated processes in Eastern Boundary current regions. Observations suggest a model resolution of at least 1 km is needed.

Cuddy formation at Cape Mendocino was observed 13 times. Two types of cuddy formation were observed, one involving a cuddy that developed in Trinidad Canyon, and the other involving floats that left the continental slope in the region of Cape Mendocino. D'Asaro (1988) suggested that "meddy" formation occurred as a consequence of separation of the Mediterranean Undercurrent (MUC) at Cape St. Vincent due to reduction of potential vorticity on the inshore side of the MUC. This was confirmed by observations of Bower et al. (1997) that relative vorticity of meddies ($-0.6f$ to $-0.3f$) were comparable to the anticyclonic shear on the inshore side of the MUC ($-0.4f$ to $-0.3f$). At Cape Mendocino, ADCP observations show a CUC core at 175 m depth and a distance of 20 km from the slope with maximum velocities of 20–30 cm/s (Pierce et al., 2000). The

anticyclonic shear between this core and the coast is −0.15 to −0.2 f. This compares well with the relative vorticity of looping for Float 67, −0.12 to −0.3 f. Hence the frictional torque mechanism observed by D'Asaro (1988) was largely responsible for eddy formation at Cape Mendocino.

Given the role of frictional torque, strong poleward flow in the CUC should be a precursor for float looping. Mean float speeds for floats which became loopers (did not loop) for Cape Mendocino were 13 ± 1.2 cm/s (7 ± 1.0 cm/s), with peak speeds for both looping and non-looping floats of ~30 cm/s. The onshore–offshore position of the float relative to the CUC core should also be important in determining the likelihood of looping. Unfortunately, this quantity was not observed in the program described here. Pierce et al. (2000) chart a series of shipboard ADCP measurements along the coast, where the offshore distance of maximum poleward flow fluctuated considerably from section to section. For example, just south of Cape Mendocino the maximum poleward flow was next to the shelf; but the average position of the flow between 38° and 43°N is 20 km from the shelf.

A second factor observed in cuddy formation was epicycloidal behavior. Epicycloidal behavior was observed in 7 of the 13 looping floats and all floats with epicycloids that moved offshore at Cape Mendocino became cuddies. The cause and origin of the epicycloidal behavior could not be determined from the float data.

The cuddies that we have observed along the U.S. West Coast are similar to the looping of RAFOS floats associated with meddies observed along the Eastern Boundary of the Subtropical Gyre in the North Atlantic. Shortly after they are formed, meddies are readily identified by their salty core of Mediterranean Water. The salty core is about 0.65 greater than the salinity of the ambient water, centered at a depth of about 1000 m, 400 m thick and 40 km in diameter (Armi et al., 1989). Meddies are much better studied than their Pacific counterparts, with multiple surveys of their density and velocity structure, and observations of their decay have been made over a period of two years (Armi et al., 1989; Schultz Tokos and Rossby, 1991). The saltly core of the meddy is in solid body rotation, with maximum velocity observed at the salt front that marks the outer edge of the core. Heat and salt are lost through a variety of mixing processes with a time (e-folding) scale of one year.

The experiment described in this paper was similar to an Atlantic Ocean experiment which seeded the Mediterranean Undercurrent (MU) in the Iberian Basin with RAFOS floats (Bower et al., 1997; Richardson et al., 2000), except that this experiment took more than a decade while the Atlantic experiment was completed in less than two years. The Iberian Basin data showed looping float behavior associated with generation of about 17 Mediterranean eddies (meddies) per year through interaction between the undercurrent and bottom topography near Cape St. Vincent and Tejo Plateau, Portugal. While there are differences between the MU and the CUC – the core of the MU is at 1000 m depth and is somewhat stronger than that of the CUC – and the geometry and features of the Iberian Basin differ somewhat from those off California – sharper capes, positions of seamounts – the latitudes and Eastern Boundary setting are similar.

Meddy properties based upon 26.8 years of RAFOS float data have been reported by Bower et al. (1997) and Richardson et al. (2000). Meddy characteristics similar to those reported for cuddies above included looping 30% of the time, a 2:1 ratio for anticyclonic vs. cyclonic looping, and a shorter duration for cyclonic vs. anticyclonic looping. Meddies were somewhat stronger and larger than cuddies, with swirl speeds of 30 cm/s for 30–60 km eddies, rotation periods from 2.5 to 17 days, and diameters from 30 to 120 km. Meddies also translated to the west in a similar manner as cuddies, with initial northward or northwestward and offshore southwestward drift. Meddy formation included epicycloidal motion prior to looping and formation due to the topographic instability at specific locations where the coastline turned sharply right when facing downstream. Finally, the timescale for meddy formation was on the order of 3–7 days. The similarity of meddies and cuddies suggests that long-lived anticyclonic eddy generation by topographic drag in poleward flows is common to Eastern Boundary currents and is not just a Mediterranean Undercurrent phenomenon alone. This is also evident in the analysis of global SSH anomalies (Chelton et al., 2011).

Four long-lived shallow cyclonic loopers were observed. They were smaller (25 km diameter) and had shorter period (10 days) than the cuddies, but had comparable swirl speeds (10 cm/s) and translation speeds (3 cm/s). Although the mean translation of the cyclonic loopers was away from the coast, their paths were unusual: three had loops and only one had northward displacement. (The cyclonic eddies observed by Chelton et al., 2011, moved northward, but had greater displacement and probably greater diameter than the loopers.) The eastward translation of the loopers is unlikely to have been caused by currents.

Long-lived eddies trapped two deep RAFOS floats, one cyclonic (1167 dbar) and the other anticyclonic (1545 dbar), to the west of Monterey Bay. The cyclonic eddy is unexpected: it cannot be caused by baroclinic processes and has not been observed in numerical model simulation (Kurian et al., 2011). Nonlinear Rossby waves are a possible explanation for this cyclone, as they can transport substances at depths greater than 1000 m (Ivanov et al., 2010). Both deep long-lived eddies ended near Taney seamounts. This fate too has been observed for meddies in the Iberian Basin (Richardson et al., 2000).

Additional studies of these looping floats are planned. A detailed examination of looper formation between Pt. Sur and Pt. Reyes will focus on the possible causes of cyclonic vs. anticyclonic rotation. For a few very long trajectories, case studies of looping behavior using wavelets, ancillary ARGO float data, and comparison of two floats that were caught in the same eddy are being completed. Shallow long-lived loopers identified in Table 1 are clearly seen in charts of sea surface height anomalies (SSHA), and kinematic properties of float trajectories and SSHA are being compared by Dudley Chelton.

Acknowledgments

These observations were sponsored by the Office of Naval Research and the Naval Postgraduate School. Newell Garfield, Skip Carter and Bob Paquette made seminal contributions to the program. L.I. and T.M. received support from the National Research Council. Support for L.I. (CC) was provided by NSF grant OCE-0827527 and DMS-1025535 (OCE-0827160). We would like to thank three anonymous reviewers and Dudley Chelton for useful comments which have considerably improved this paper. We would also like to thank Tom Rossby for his many contributions to observational oceanography, including those which have made this study possible.

(T.A.R.) Tom was the kind of thesis advisor everyone should have had, although that isn't always entirely obvious to the advisee at the time. Tom always knew when to step in with sage advice and guidance. But, possibly more importantly, he also knew when to leave his charge alone to figure things out for himself. A perfect example came during my first Pegasus cruise with Tom. After demonstrating once (or maybe twice—I do not remember) how not to lose the expensive instrument and maneuver the ship for recovery, Tom proceeded to hand the reins over to his two newest students, then completely disappeared from the lab. After some initial panic, we figured out how to get the instrument back—as, of course, Tom knew all along we would.

(C.A.C.) I first met Tom as a participant in the Mid Ocean Dynamics Experiment (MODE) in 1972. Tom was rather quiet compared to the average MODE PI, and the only incident I remember is when Tom's long-haired technician found that he could hear the SOFAR floats much better when he used a classified hydrophone array. This was promptly discovered by a Navy Chief, and the resulting confrontation came near to sinking the SOFAR float program. (With help from ONR, reason prevailed. But the technician became *persona non grata* at Navy SOSUS facilities.) Later, in 1987, one of Tom's thesis students (Tarry Rago) and postdocs (Skip Carter) joined NPS and were essential in making measurements of CUC kinematics using Pegasus and RAFOS floats, respectively, instrument systems that Tom had developed. The sound sources used in the NPS RAFOS program were originally purchased as SOFAR floats, but were quickly converted to sources. So, Tom also deserves some credit for the extra 55 float-years of data acquired, some of which are described here.

Appendix A. Probability distribution functions (PDFs) for eddy characteristics

Because of the small number of samples available, the method developed by Ivanov and Tokmakian (2011) was used to reconstruct PDFs for anticyclonic looper characteristics. The method represents a distribution as a finite mixture of P modes

$$f(\tau) = \sum_{p=1}^{P} \lambda_p f_p(\tau), \quad (1)$$

where λ_p is the relative abundance of the pth component (mode) as a proportion of the total sampling, and must satisfy the constraints $0 \le \lambda_p \le 1$ and $\sum_{p=1}^{P} \lambda_p = 1$, and f_p is the distribution for the pth mode. If $P=1$, $f(\tau)$ is a uni-modal distribution. Mathematical details for finite mixture models as (1) can be found in McLaughlan and Peel (2000).

Each mode in (1) was reconstructed separately from specially constructed subsamples using a variational method developed in Ivanov and Chu (2007). The final step of the procedure determines λ_p in (1) through an expectation-minimization algorithm (McLaughlan and Peel, 2000). Reconstruction skill of the distribution function is controlled through the mismatch between the reconstructed cumulative distribution function (CDF) corresponding to (1) and the empirical CDF obtained directly from original re-sampling.

The non-Gaussian character of distributions for anticyclonic loopers shown in Fig. 8A, B and D is shown by asymmetric pdfs that are bounded by abscissa values of zero on the left and have long tails that approach ordinate values of zero on the right. The pdf for the translation velocity (Fig. 8D) is very close to a three parameter Weibull distribution,

$$f(x|\gamma,\beta,\alpha) = \gamma\beta^{-\gamma}(x-\alpha)^{\gamma-1} \ \exp\left[-\left(\frac{x-\alpha}{\beta}\right)^{\gamma}\right]$$

for which $\alpha=1.7$ cm/s, $\beta=2/2$ cm/s and $\gamma=0.1$. The distribution for anticyclonic looper period (Fig. 8B) and translation direction (Fig. 8E) were bimodal; for period $\lambda_1=0.8$, $\lambda_2=0.2$ and for direction $\lambda_1=0.85$ and $\lambda_2=0.15$.

References

Armi, L., Hebert, D., Oakey, N., Price, J., Richardson, P., Rossby, T., Ruddick, B., 1989. Two years in the life of a Mediterranean salt lens. J. Phys. Oceanogr. 19, 354–370.

Barth, J.A., Pierce, S.D., Smith, R.L., 2000. A separating coastal upwelling jet at Cape Blanco, Oregon and its connection to the California Current System. Deep-Sea Res. II 47, 783–810.

Benson, K., 1995. High Frequency Subsurface Lagrangian Measurements in the California Current with RAFOS Floats. M.S. Thesis, Naval Postgraduate School, Monterey, CA, 88 pp. 〈http://www.oc.nps.navy.mil/npsRAFOS/BENSONthesisPDF.pdf〉.

Boebel, O., Schultz Tokos, K.L., Zenk, W., 1995. Calculation of salinity from neutrally buoyant RAFOS floats. J. Atmos. Ocean. Technol. 12, 923–934.

Boebel, O., Lutjeharms, J., Schmid, C., Zenk, W., Rossby, T., Barron, C., 2003. The Cape Cauldron: a regime of turbulent inter-ocean exchange. Deep-Sea Res. II 50, 57–86.

Bower, A.S., Armi, L., Ambar, I., 1997. Lagrangian observations of Meddy formation during a Mediterranean undercurrent seeding experiment. J. Phys. Oceanogr. 27, 2545–2575.

Bray, N.A., Keyes, A., Morawitz, W.M.L., 1999. The California Current system in the Southern California Bight and the Santa Barbara Channel. J. Geophys. Res. 104, 7695–7714.

Chelton, D.B., Schlax, M.G., Samelson, Roger M., 2011. Global observations of nonlinear mesoscale eddies. Prog. Oceanogr. 91, 167–216, http://dx.doi.org/10.1016/j.pocean.2011.01.002.

Chereskin, T.K., Morris, M.Y., Niiler, P.P., Kosro, P.M., Smith, R.L., Ramp, S.R., Collins, C.A., Musgrave, D.L., 2000. Spatial and temporal characteristics of the mesoscale circulation of the California Current from eddy-resolving moored and shipboard measurements. J. Geophys. Res. 105, 1245–1269.

Collins, C.A., Paquette, R.G., Ramp, S.R., 1996. Annual variability of ocean currents at 350 m depth over the continental slope off Pt. Sur, California. CalCOFI Reports 73, 1–7.

Collins, C.A., Garfield, N., Rago, T.A., Rischmiller, F.W., Carter, E., 2000. Mean structure of the inshore countercurrent and California undercurrent off Pt. Sur, California. Deep-Sea Res. II 47, 765–782.

Collins, C.A., Ivanov, L.M., Melnichenko, O.V., Garfield, N., 2004, California Undercurrent variability and eddy transport estimated from RAFOS float observations, J. Geophys. Res., 109, C05028, http://dx.doi.org/10.1029/2003JC002191.

D'Asaro, E., 1988. Generation of submesoscale vortices: a new mechanism. J. Geophys. Res. 93 (C6), 6685–6693.

Flament, P., 2002. A state variable for characterizing water masses and their diffusive stability: spiciness. Prog. Oceanogr. 54, 493–501.

Flierl, G., 1981. Particle motion in large-amplitude wave fields. Geophys. Astrophys. Fluid Dyn. 18, 39–74.

Garfield, N., Collins, C.A., Paquette, R.G., Carter, E., 1999. Lagrangian exploration of the California Undercurrent, 1992–1995. J. Phys. Ocean 29, 560–583.

Garfield, N., Maltrud, M., Collins, C.A., Rago, T.A., Paquette, R.G., 2001. Lagrangian flow in the California Undercurrent, and observation and model comparison. J. Mar. Syst. 29, 201–220.

Hickey, B.M., 1989. Patterns and processes of circulation over the Washington continental shelf and slope. In: Coastal Oceanography of Washington and Oregon, Elsevier Oceanography Series, vol. 47, pp. 41–116.

Ivanov, L.M., Eremeev, V.N., 1987. Tracers in the ocean. Naukova Dumka.

Ivanov, L.M., Chu, P.C., 2007. On stochastic stability of regional ocean models with uncertainty in wind forcing. Nonlinear Proc. Geophys. 14, 655–670.

Ivanov, L.M., Collins, C.A., Margolina, T.M., Piterbarg, L.I., Eremeev, V.N., 2008. On westward transport processes off central California revealed by RAFOS floats. Geophys. Res. Lett. 35, L18604, http://dx.doi.org/10.1029/2008GL034689.

Ivanov, L.M., Collins, C.A., Marchesiello, P., Margolina, T.M., 2009. On model validation for meso/submesoscale currents: metrics and application to ROMS off Central California. Ocean Modell. 28, 209–225.

Ivanov, L.M., Collins, C.A., Margolina, T.M., Eremeev, V.N., 2010. Nonlinear Rossby waves off California. Geophys. Res. Lett. 37, L13602, http://dx.doi.org/10.1029/2010GL043708.

Ivanov, L.M., Tokmakian, R.T., 2011. Sensitivity analysis of nonlinear models to parameter perturbations for small size ensembles of model outputs. I. J. Bifur. Chaos 21 (12), 3589–3609.

Keister, J.E., Strub, P.T., 2008. Spatial and interannual variability in mesoscale circulation in the northern California Current System. J. Geophys. Res. 113 (C04015), http://dx.doi.org/10.1029/2007JC004256.

Kelly, K.A., Beardsley, R.C., Limeburner, R., Brink, K.H., Paduan, J.D., Chereskin, T.K., 1998. Variability of the near-surface eddy kinetic energy in the California Current based on altimetric, drifter and moored current meter data. J. Geophys. Res. 103, 13067–13083.

Kurian, J., Colas, F., Capet, X., McWilliams, J.C., Chelton, D.B., 2011. Eddy properties in the California Current System. J. Geophys. Res. 116, C08027, http://dx.doi.org/10.1029/2010JC006895.

Lukas, R., Santiago-Mandujano, F., 2001. Extreme water mass anomaly observed in the Hawaii ocean time-series. Geophys. Res. Lett. 28 (15), 2931–2934.

Lupton, J.E., Baker, E.T., Garfield, N., Massoth, G.J., Feely, R.A., Cowen, J.P., Greene, R.R., Rago, T.A., 1998. Tracking the evolution of a hydrothermal event plume with a RAFOS neutrally buoyant drifter. Science, 1052–1055, http://dx.doi.org/10.1126/science.280.5366.1052.

Margolina, T., Collins, C.A., Rago, T.A., 2006. Intermediate level Lagrangian subsurface measurements in the northeast Pacific: isobaric RAFOS float data, 2006. Geochem. Geophys. Geosyst. 7 (9), Q09002, doi:10.129/2006GC001295.

McLaughlan, G.J., Peel, D., 2000. Finite Mixture Models. Wiley, New York, 419 pp.

Pierce, S.D., Smith, R.L., Kosro, P.M., Barth, J.A., Wilson, C.D., 2000. Continuity of the poleward undercurrent along the eastern boundary of the mid-latitude north Pacific. Deep-Sea Res. II 47, 783–810.

Regier, L., Stommel, H., 1979. Float trajectories in simple kinematic flows. Proc. Nat. Acad. Sci. U.S.A. 76, 1760–1764.

Richardson, P.L., 1993. A census of eddies observed in North Atlantic SOFAR float data. Prog. Oceanogr 31, 1–50.

Richardson, P.L., Bower, A.S., Zenk, W., 2000. A census of Meddies tracked by floats. Prog. Oceanogr. 45, 209–250.
Rossby, T., Dorson, D., Fontaine, J., 1986. The RAFOS system. J. Atmos. Ocean. Technol. 3, 672–679.
Schultz Tokos, K., Rossby, T., 1991. Kinematics and dynamics of a Mediterranean salt lens. J. Phys. Oceanogr. 21, 879–892.
Schlax, M., Chelton, D.B., 2008. The influence of mesoscale eddies on the detection of quasi-zonal jets in the ocean. Geophys. Res. Lett. 35, L24602, http://dx.doi.org/10.1029/2008GL035998.
Shoosmith, D.R., Richardson, P.L., Bower, A.S., Rossby, H.T., 2005. Discrete eddies in the northern North Atlantic as observed by looping RAFOS floats. Deep-Sea Res. II 52, 627–650.
Simpson, J.J., Lynn, R.J., 1990. A mesoscale eddy dipole in the offshore California Current. J. Geophys. Res. 95 (C8), 13009–13022.
Stegmann, P.M., Schwing, F., 2007. Demographics of mesoscale eddies in the California Current. Geophys. Res. Lett. 34 (L14602), 4, http://dx.doi.org/10.1029/2007GL029504.
Swift, D.D., Riser, S.C., 1994. RAFOS floats: defining and targeting surfaces of neutral buoyancy. J. Atmos. Ocean. Technol. 11, 1079–1092.
Sverdrup, H.U., 1939. Physics and Geophysics with Special Reference to Problems in Physical Oceanography. University of California Press, Berkeley, CA, 23 pp.
Zamora, U.D., 2009. An Atlas of Deep Current Measurements for Central California. M.S. Thesis, Naval Postgraduate School, 266 pp.